Institut für Veterinärpharmakologie und -toxikologie
der Vetsuisse-Fakultät Universität Zürich
Direktor: Prof. Dr. Felix R. Althaus

Arbeit unter Leitung von Dr. Ulrike Camenisch

Establishment and application of fluorescence recovery after photobleaching to study the nuclear dynamics of DNA repair proteins

Inaugural-Dissertation

zur Erlangung der Doktorwürde der
Vetsuisse-Fakultät Universität Zürich

vorgelegt von

Renée Müller

Tierärztin
von Hoyerswerda, Deutschland

genehmigt auf Antrag von
Prof. Dr. Hanspeter Nägeli, Referent
PD Dr. Andreas Luch, Korreferent

Zürich 2010

TABLE OF CONTENTS

LIST OF ABBREVIATION

6-4 PP	Pyrimidine (6-4) pyrimidone photoproduct
BER	Base excision repair
DMEM	Dulbecco's Modified Eagle medium
CHO	Chinese hamster ovary
CNT	Centrin 2
CPD	Cyclobutane pyrimidine dimer
CS	Cockayne syndrome
DDB	DNA-binding protein
DNA	Deoxyribonucleic acid
DPX	DNA-protein crosslink
DsRed	Red fluorescent protein from *Discosoma* sp.
ECFP	Enhanced cyan fluorescence protein
EGFP	Enhanced green fluorescence protein
ERCC1	Excision repair cross-complementing 1
EYFP	Enhanced yellow fluorescence protein
FA	Formaldehyde
FBS	Fetal bovine serum
FRAP	Fluorescence recovery after photobleaching
GFP	Green fluorescence protein
GGR	Global genome repair
IARC	International Agency for Research on Cancer
mRFP	Monomeric red fluorescence protein
NER	Nucleotide excision repair
PBS	Phosphate-buffered saline
RAD23B	RAD23 homolog B
ROI	Region of interest
RPA	Replication protein A
TCR	Transcription-coupled repair
TFIIH	Transcription factor IIH
Ub	Ubiquitin
UV	Ultraviolet
wt	Wild-type

XP	Xeroderma pigmentosum

1 SUMMARY

The genetic information is constantly exposed to physical and chemical DNA-damaging agents. To safeguard genome stability, nucleotide excision repair (NER) is a protective system that processes a wide diversity of structurally unrelated DNA lesions, including UV-induced photoproducts and cisplatin intrastrand crosslinks. The aim of this thesis was to establish novel fluorescent protein-based imaging techniques to study NER activity in living fibroblasts and to apply these methods to determine the mechanism by which low-dose formaldehyde, a widely used genotoxic chemical, inhibits DNA repair. The nuclear movements of NER factors were analyzed by measuring the kinetics of accumulation at lesion sites and by monitoring protein dynamics in fluorescence recovery after photobleaching (FRAP) experiments. In combination, this live-cell imaging approach reveals that formaldehyde, at non-cytotoxic concentrations, impedes the intra-nuclear trafficking of the DNA damage recognition proteins DDB2 and XPC, thus retarding their recruitment to NER substrates. Further live-cell imaging experiments with fluorescently tagged ubiquitin suggest that DDB2 stimulates protein ubiquitylation in response to formaldehyde exposure. In conclusion, these findings indicate that formaldehyde-induced DNA-protein crosslinks interfere with the normal trafficking of NER subunits, thus distracting these repair factors from their physiologic function in recognizing and processing mutagenic DNA lesions.

2 INTRODUCTION

2.1 Live cell imaging

For many years, the properties and activities of isolated proteins have been extensively studied under defined experimental conditions *in vitro*. However, such biochemical systems are not directly comparable to the situation in a living cell or organism, where proteins act in a complex macromolecular environment. Therefore, it is crucial to understand how proteins behave not only in isolation but also in this physiologic context *in situ* (Gierasch & Gershenson 2009). In particular, great efforts have been undertaken during the last years to visualize proteins in their intrinsic environment by fusing them to genetically encoded fluorescent tags (Chalfie *et al.* 1994).

Live cell imaging of fluorescently tagged molecules is a powerful new experimental approach that allows for the real-time monitoring of complex biological events. In combination with concurrent biochemical and structural studies on the proteins of interest, live cell imaging provides the opportunity to monitor the consequences of macromolecular interactions, posttranslational protein modifications and protein conformational changes that have been determined in vitro either with purified factors or various cell extracts. As a consequence, the imaging of fluorescently tagged proteins has become an essential tool to study protein kinetics and dynamics within the complex micro-environment of living cells (Day *et al.* 2006; Day & Schaufele 2008).

2.1.1 Fluorescent proteins

In 2008, Prof. Osamu Shimomura, Prof. Martin Chalfie and Prof. Roger Tsien were awarded the Nobel Prize in Chemistry for their work on fluorescent proteins. The green-fluorescent protein (GFP) in association with the blue light-emitting aequorin was first isolated from the jellyfish *Aequora victoria* by Prof. Shimomura. He found that the binding of calcium ions to aequorin leads to the release of blue light. The GFP partner absorbs the blue light and in turn emits a green-fluorescent signal (Shimomura *et al.* 1962; Shimomura *et al.* 1963; Morise *et al.* 1974).The 238 amino

acids of GFP assemble into a compact cylindrical structure, resembling a barrel, that is capped on both ends by short α-helical sections. This three-dimensional protein fold is crossed by another α-helix that includes the amino acid sequence Ser65-Tyr66-Gly67, which builds the chromophore center involving an autocatalytic cyclization of the Tyr66 residue (Shimomura 1979; Ormö *et al.* 1996; Yang *et al.* 1996). The chromophore is intrinsic to the primary structure of the GFP protein and the resulting fluorescence can only be detected when the chromophore is embedded within the complete GFP sequence (Li *et al.* 1997). After the initial cloning and complementary DNA sequencing, the group of Prof. Chalfie expressed GFP in *E. coli* and *C. elegans*, demonstrating that it can be used as a molecular tag to visualize specific proteins in living cells and whole organisms (Chalfie *et al.* 1994). Subsequent modifications of the original GFP amino acid sequence yielded a wide range of variants with different colors and improved photo-physical properties (Heim & Tsien 1996). The enhanced GFP (EGFP) carries two amino acid substitutions shifting the major excitation peak from ~400 nm to ~490 nm wavelength. The argon-ion laser routinely used in confocal scanning laser microscopes emits at 488 nm yielding a much more efficient excitation of EGFP compared to the wild-type GFP (Cormack *et al.* 1996; Yang *et al.* 1996). Other widely used spectral variants included enhanced yellow-fluorescent protein (EYFP) and enhanced cyan-fluorescent protein (ECFP). EYFP contains four amino acid substitutions that shift the emission from green to yellowish-green. One of the amino acid substitutions in the ECFP sequence shifts the emission spectrum from green to cyan, while the other five mutations enhance the brightness and solubility of the protein (Heim & Tsien 1996).

The color palette of fluorescent proteins was expanded by the discovery of a new red-shifted species, DsRed, from the coral *Discosoma* sp. (Matz *et al.* 1999). The chromophore of this red homolog of GFP has an extra double bond, which is responsible for the red shift (Gross *et al.* 2000). However, the slow and incomplete maturation and obligate tetramerization of DsRed greatly hindered its use as a fusion tag (Baird *et al.* 2000). Meanwhile, an improved monomeric variant of red fluorescent protein (mRFP) has been engineered (Campbell *et al.* 2002; Bevis & Glick 2002).

2.1.2 Fluorescence recovery after photobleaching

The fluorescence recovery after photobleaching (FRAP) technique has been developed to study the real-time dynamics of biomolecules in living cells (Edidin *et al*. 1976). This method is, for example, a very useful tool to estimate the bound fraction of a protein compared to the freely diffusing counterparts in a given biological compartment. In the context of this thesis, FRAP is used to determine the DNA damage-induced changes in the mobility of DNA repair factors. In FRAP, the fluorescent tag of the fusion protein is irreversibly bleached within a defined area of interest of the cell or any other cellular compartment. Thereafter, the gradual recovery of fluorescence in the bleached area, taking place by protein diffusion, is monitored over a particular period of time. The final output of this real-time analysis is a display of the time course of fluorescence recovery, which reflects the proportion of mobile and immobile fractions of the protein (Figure 1). When all tagged molecules are freely mobile, there will be a complete recovery of fluorescence in the bleached region. If, on the other hand, all tagged molecules were immobile, no fluorescence recovery would be observed and the bleached area would remain dark. In the more frequent intermediate situation, fluorescence in the bleached area will partly recover, such that the percentage of recovery is a measure for the mobility of the tagged molecules. The respective immobile fraction represents a snapshot of a steady state binding equilibrium due to interactions with cellular structures (Cardarelli *et al*. 2009; van Royen *et al*. 2009; Kalla *et al*. 2006; Carrero *et al*. 2003).The example of Figure 1 shows a typical FRAP experiment performed in human fibroblasts expressing a GFP-tagged protein that is localized to the cell nucleus. The advanced technical requirements needed to perform this fluorescence-based live cell imaging technique includes a confocal microscope to clearly visualize a single optical plane in the three-dimensional scaffold of living cells without any interference due to out-of-focus signals.

(A)

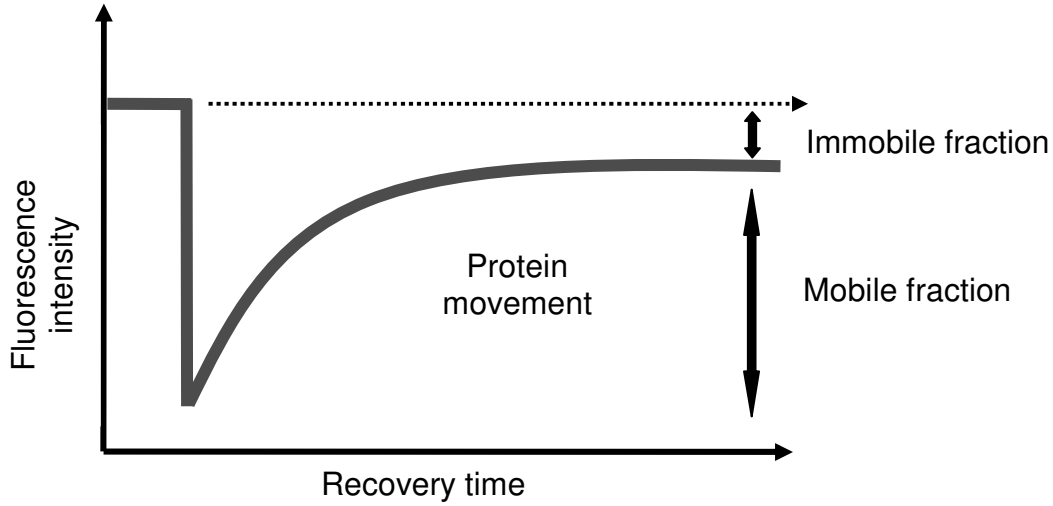

(B)

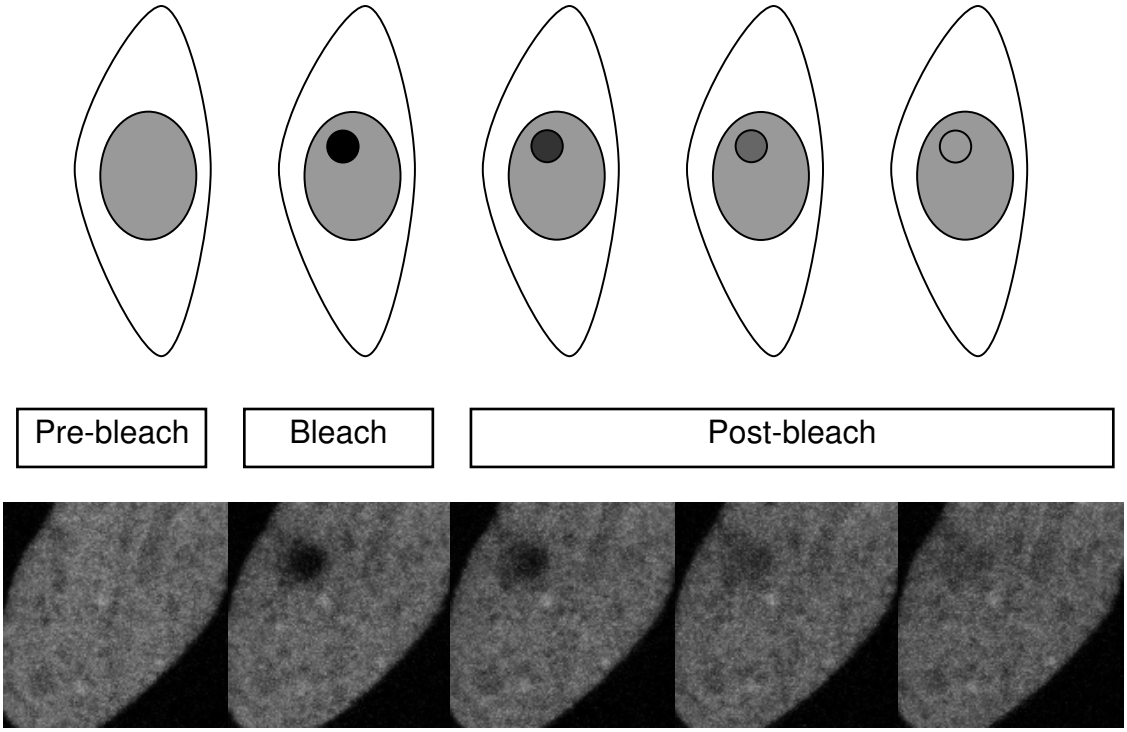

Figure 1: *Example of a FRAP experiment in human fibroblasts expressing a GFP-tagged nuclear protein. (A) Representative plot showing the protein dynamics resulting from its mobile and immobile fractions. (B) Schematic description of the FRAP procedure with the respective real-time images of a cell expressing the GFP tagged protein. Prebleach = before exposure to the argon laser (488 nm wavelength); bleach = irradiation of the ROI; postbleach = recovery of fluorescence after local bleaching.*

2.2 Maintenance of genomic stability

Deoxyribonucleic acid (DNA) is the carrier of the genetic information. Although its long-term integrity is indispensable for the survival of cells, organisms and entire species, the DNA is continuously exposed to the damaging effects of several harmful endogenous and exogenous agents such as oxidative radicals, UV light, X-rays and electrophilic chemicals. These genotoxic insults cause a number of adverse consequences in the form of DNA damage: double strand breaks, single strand breaks, base modifications, base losses as well as photoproducts, DNA adducts, intrastrand or interstrand crosslinks and DNA-protein crosslinks (Greene 1992; Sancar 1996; Wood 1997; Barker *et al*. 2005; Friedberg *et al*. 2006; Lopes *et al*. 2006). If left unrepaired, these DNA lesions may lead to cell death or, alternatively, to the accumulation of mutations eventually triggering the development of a tumor (Sancar 1996; Wood 1997). To avoid these detrimental consequences of DNA damage, mammalians developed various repair pathways. For example, double strand breaks are patched by homologous recombination or non-homologous end-joining (Li & Heyer 2008; Yano *et al*. 2009) and oxidative base modifications are mainly processed by base excision repair (BER) (Baute & Depicker 2008). The present thesis is focused on the nucleotide excision repair (NER) pathway that is characterized by its capacity to recognize a broad range of lesions including UV photoproducts, DNA adducts and intrastrand DNA crosslinks.

2.2.1 Nucleotide excision repair

As mentioned before, the NER pathway detects and processes a large diversity of structurally unrelated lesions, including bulky damages such as UV light-induced photoproducts, bulky oxidative lesions, carcinogen-DNA adducts and cisplatin-induced intrastrand DNA crosslinks. All these NER substrates share the common property to distort the helical conformation of the DNA double helix (Satoh *et al*. 1993; Reardon *et al*. 1997; Kuraoka *et al*. 2000; Dip *et al*. 2004; Reardon *et al*. 2006; Shivji *et al*. 2006).

Defects in the NER pathway have been discovered in individuals suffering from the inherited syndromes Xeroderma pigmentosum (XP), Cockayne syndrome (CS) and

Trichothiodystrophy (de Boer & Hoeijmakers 2000). XP is a rare autosomal recessive disorder in humans. This genetic disease is mainly characterized by an extreme hypersensitivity to sunlight and a 2000-fold increased incidence of skin cancer, mainly squamous cell carcinomas, basal cell carcinomas and melanomas (Kraemer *et al*. 1984; Friedberg *et al*. 2006). XP patients also suffer from a higher risk of contracting internal tumors, in some cases combined with neurological complications (Satoh *et al*. 1993; D´Errico *et al.* 2006). Individuals affected by XP are classified in 7 NER-deficient complementation groups designated XP-A through XP-G, which reflect mutations in distinct repair genes (Sancar 1996; Wood 1996; Andressoo *et al*. 2005). The respective NER proteins (XPA through XPG) were named after the corresponding genetic complementation group.

2.2.1.1 Global genome repair

The NER system can be subdivided in two sub-pathways, “global-genome repair” (GGR) and “transcription-coupled repair” (TCR). The GGR sub-pathway removes DNA lesions from anywhere in the genome, whereas TCR only removes DNA damage from actively transcribed sequences (Hanawalt 2002; Maddukuri *et al*. 2007; Nouspikel 2009). Although many mechanistic details are still highly debated, a favored model proposes that these repair machineries are assembled on damaged DNA sites in a sequential manner. In particular, the GGR sub-pathway is initiated by the binding of XPC protein, together with RAD23B and the calcium-binding protein centrin 2 (CNT2), to target lesions as illustrated in Figure 2 (Volker *et al*. 2001; Nishi *et al*. 2005). The XPC subunit is able to detect damage-induced distortions of the DNA double helix by sensing abnormal strand oscillations (Sugasawa *et al*. 1998; Buterin *et al*. 2005; Maillard *et al*. 2007). The other components of the trimeric XPC complex, RAD23B and CNT2, stimulate GGR activity by stabilizing the XPC subunit via protection from proteasomal degradation and by promoting its DNA-binding function (Ng *et al*. 2003). After the recognition of damaged sites by the XPC complex, the GGR pathway proceeds by the recruitment of transcription factor TFIIH, a large factor consisting of 10 subunits that includes the two DNA helicases XPB and XPD. Using its DNA helicase subunits, TFIIH unwinds the damaged site by 20-25 nucleotides generating an open intermediate (Mu *et al*. 1997). This local unwinding of

the duplex generates double-stranded to single-stranded DNA junctions at the edges of a central bubble, thus providing a preferred incision substrate for the two structure-specific endonucleases XPF-ERCC1 and XPG (Drapkin & Reinberg 1994; O´Donovan *et al*. 1994; Bessho *et al*. 1997; Bienstock *et al*. 2003). The term ERCC1 (for excision-repair-cross-complementing 1) denotes an interaction partner of XPF that is absolutely required for its stability and nuclease activity (Enzlin & Schärer 2002).

It has been reported that XPA and replication protein A (RPA) become incorporated into the nascent NER complex following the recruitment of TFIIH, whereas XPC-RAD23B-CNT2 is displaced from the ultimate pre-incision intermediate (You *et al*. 2003). The function of XPA protein is controversially discussed, but the proper association of XPA with the DNA intermediate is required for the assembly of a productive incision complex (Camenisch *et al*. 2006; Camenisch *et al*. 2007). Furthermore, XPA interacts with RPA, a single-stranded DNA-binding protein that protects the undamaged complementary strand from accidental endonucleolytic cleavage (de Laat *et al*. 1998). XPA and RPA, in combination, also provide a docking platform for XPG and XPF-ERCC1 (Matsunga *et al*. 1995; Mu *et al*. 1997). XPG performs the 3' incision and the XPF-ERCC1 heterodimer is responsible for the 5' incision. This dual incision reaction leads to the release of an oligonucleotide segment containing the offending DNA damage. The resulting single-stranded gap is filled by a DNA polymerase (δ, ε or κ) using the undamaged complementary strand as a template (Shivji *et al.* 1995; Araújo *et al*. 2000). Finally, the remaining nick between the newly synthesized DNA repair patch and the pre-existing strand is sealed by the action of DNA ligases.

Figure 2: *Scheme of the GGR pathway with the star symbolizing an offending DNA lesion. The following core NER factors are responsible for the GGR response in human cells: XPC-RAD23B-CNT2, TFIIH (containing the DNA helicases XPB and XPD), XPF-ERCC1, XPG, XPA, RPA, a DNA polymerase (POLδ, POLε or POLκ) and DNA ligases (see text for references). An accessory factor referred to as DDB (for damaged DNA-binding) stimulates the recognition and repair of UV lesions (Keeney et al. 1994; Hwang et al. 1999; Tang et al. 2000; Fitch et al. 2003; Moser et al. 2005)*

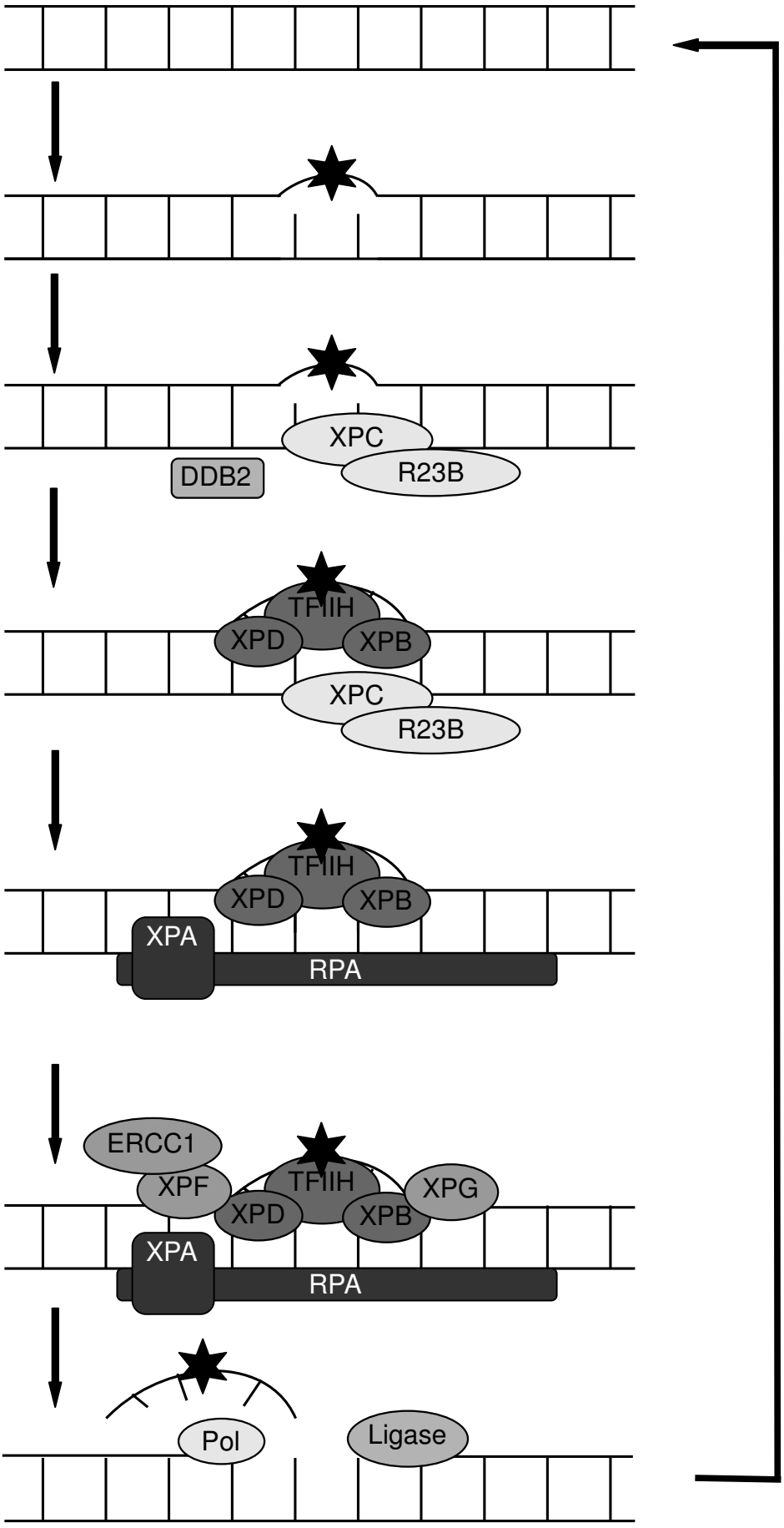
XPC
R23B
DDB2
TFIIH
XPD
XPB
XPC
R23B
TFIIH
XPD
XPB
XPA
RPA
ERCC1
XPF
TFIIH
XPG
XPD
XPB
XPA
RPA
Pol
Ligase

2.2.1.2 Transcription-coupled repair

Unrepaired DNA lesions not only lead to the accumulation of genetic mutations but also interfere with the ongoing transcriptional process. The resulting inhibition of gene functions triggers cell cycle arrest, cell senescence (a permanent cell cycle block) or cell death by apoptosis (Mitchell *et al*. 2003). To prevent these adverse effects of DNA damage, living organisms have developed a transcription-coupled repair (TCR) sub-pathway that removes DNA lesions selectively from the transcribed strand of active genes. TCR is initiated when the RNA polymerase II complex stalls in the proximity of the lesions, followed by the sequential recruitment of TFIIH, XPA, RPA as well as XPG and XPF-ERCC1. XPC-RAD23B-CNT2, the key recognition factor in GGR, is dispensable for the TCR pathway (Venema *et al*. 1991; van Hoffen *et al*. 1995). Instead, the TCR reaction depends on the two Cockayne syndrome (CS) genes, *CSA* and *CSB*. Several models of the TCR pathway propose that CSB protein interacts with the lesion-stalled RNA polymerase (Sarasin & Stary 2007) and then recruits other repair factors to the damaged site, including CSA which is part of an E3-ubiquitin ligase complex consisting of the three proteins DDB1, Cullin 4A and ROC1/Rbx1 (Groisman *et al*. 2003, Fousteri *et al*. 2006).

2.3 DNA lesions

The presence of multiple repair pathways reflects the susceptibility of DNA to damage by various genotoxic insults (Camenisch & Naegeli 2009; Nouspikel 2009). In fact, DNA is not an intrinsically stable molecule and is subjected to constant attacks by a variety of endogenous and exogenous DNA-damaging agents. As outlined before, the NER pathway recognizes and repairs a remarkably broad range of lesions including UV photoproducts, certain oxidative lesions, carcinogen-DNA adducts and intrastrand DNA crosslinks. The same NER pathway has also been implicated in the removal of DNA-protein crosslinks (DPXs) (Reardon & Sancar 2006; Ide *et al*. 2008). Next, I will review shortly the NER substrates that are relevant for the present thesis.

2.3.1 UV light-induced DNA photoproducts

UV light is defined as electromagnetic radiation, with wavelength between 100 and 400 nm, which is commonly subdivided into three ranges. UV-B is confined to 280 – 315 nm, followed by UV-A with 315 – 400 nm. Both spectra penetrate at least in part through the atmospheric ozone layer and can be absorbed by the human skin (Mouret *et al*. 2006). Instead, the high-energy UVC range (100 to 280 nm) is entirely blocked by the ozone in the atmosphere and, therefore, does not reach the earth's surface. Dependending on the wavelength, exposure to UV radiation results in the formation of oxidative damage and two major classes of photoproducts, *i.e*., cyclobutane pyrimidine dimers (CPDs) and pyrimidine (6-4) pyrimidone photoproducts (6-4 PPs) (Pfeifer 1997; Meador *et al*. 2000; Mouret *et al*. 2006). By direct excitation, UV-C and UV-B induce the same pattern of DNA damages, namely CPDs and 6-4PPs, but the generation of CPDs occurs at ~4 fold higher frequency compared to 6-4PPs (Meador *et al*. 2000). UVA has been shown to induce oxidative damage and CPDs by an indirect mechanism involving the excitation of endogenous photo-sensitizers (Kielbassa *et al*. 1997; Perdiz *et al*. 2000). In human cells, photoproducts are solely removed via the NER pathway. UV light-induced CPDs, in comparison to 6-4PPs, cause only small distortions of the helical conformation (Kim *et al*. 1995; McAteer *et al*. 1998). As a consequence CPDs are only poorly recognized by XPC protein, the key initiator complex of the GGR pathway (Sugasawa *et al*. 2001; Kusumoto *et al*. 2001). Hence, in mammals, an accessory protein is needed for the efficient recognition and removal of CPDs from the genome (Hwang *et al.* 1999; Tang *et al.* 2000). This accessory factor specialized on the recognition of UV lesions has been discovered by virtue of its pronounced affinity for UV-irradiated DNA (Hirschfeld *et al.* 1990; Keeney *et al.* 1994) and is usually referred to as DDB (for damaged DNA-binding). It has been suggested that DDB acts by accelerating the recruitment of XPC protein to UV lesions (Fujiwara *et al*. 1999; Fitch *et al.* 2003; Moser *et al*. 2005). DDB is a heterodimer that consists of DDB1 (127 kDa) and DDB2 (48 kDa), with the smaller subunit being encoded by the *XPE* gene (Rapić-Otrin *et al.* 2003). DDB1 forms a molecular adapter for the Cul4A-Roc1 ubiquitin ligase complex (Shiyanov *et al.* 1999) and mediates the ubiquitylation of target proteins comprising DDB2 itself (Nag *et al*. 2001) and XPC protein (Sugasawa *et al.* 2005).

2.3.2 Cisplatin

Cisplatin has been used in the context of this thesis as a well characterized alkylating agent that induces DNA lesions recognized by the human NER system. It is a chemotherapeutic drug widely used for the treatment of many malignant tumors in both human and veterinary medicine (Cohen & Lippard 2001). Cisplatin generates a variety of structural modifications in DNA, the most abundant being intrastrand crosslinks formed between adjacent purine bases. A minor fraction of cisplatin-DNA lesions consists of interstrand crosslinks, i.e., covalent bonds between the two complementary strands (Sanderson *et al*. 1996; Moggs *et al*. 1997; Siddik 2003; Rabik & Dolan 2006). Intrastrand cisplatin crosslinks are removed slowly by the NER pathway (Moggs *et al*. 1996; Furuta *et al.* 2002; Chen *et al.* 2003). The process of homologous recombination is thought to participate in the removal of the interstrand crosslinks (Bergstralh & Sekelsky 2008; Mladenova & Russev 2008).

2.3.3 Formaldehyde

Formaldehyde (FA; chemical structure: HCHO) is a physiologic metabolite that is formed as a by-product of methionine and choline degradation and as an intermediate of synthesis of amino acids, purines and pyrimidines. The normal FA concentration in human blood plasma has been reported in the range of 13-97 µmol/l (Szarvas *et al.* 1986; Heck *et al.* 1985). There are also many exogenous FA sources. For example, this strong smelling flammable and colorless gas, which is soluble in water, is utilized for disinfection and tissue conservation. It is also employed as a preservative in many cosmetics. FA is widely used by industry to fabricate numerous household products and various building materials that include insulation and pressed wood products containing urea-formaldehyde resins. FA can also be found as a component in natural products like wood, apples and pears. Combustion of wood, kerosene and natural gas as well as tobacco releases FA into the environment (Emri *et al.* 2004; Heck & Casanova 2004; IARC 2004; Naya & Nakanishifehlen 2005). To estimate the extent of FA air pollution, indoor and outdoor air concentrations have been measured in an Italian city. The indoor value (0.016 ppm) was clearly higher than the concentration (0.006 ppm) measured in the outdoor air

(Fuselli *et al*. 2006). Air levels higher than 0.1 ppm cause irritation of eyes, nose and throat and provoke allergic reactions mainly of the skin (CPSC 1997). Previous studies have shown that FA displays genotoxic and mutagenic properties in mammalian cells (Ma & Harris 1988; Conaway *et al.* 1996; IARC 2004). In 2004, FA was classified by the International Agency for Research on Cancer (IARC) as carcinogen to humans (group 1) based on the significantly increased risk for nasopharyngeal cancer found in several cohort and case-control studies with industrial workers (Vaughan *et al*. 2000; Hauptmann *et al*. 2004). There is also a correlation between leukemia and occupational FA exposure (IARC 2004; Hauptmann *et al*. 2003). In rodent studies, exposure to FA by inhalation induced squamous cell carcinomas in the nasal cavities of the animals (Casteel *et al.* 1987). FA is taken up by food, absorbed through the skin or inhaled. In rats, it has been shown that 90% of FA is deposited in the upper respiratory tract after long-term inhalation (Dallas *et al*. 1985; Heck *et al*. 1985). However, blood FA levels did not change after inhalation exposure in rats, monkeys or humans (Casanova *et al*. 1988; Heck *et al*. 1983, 1985), most probably due to a rapid metabolism in the respiratory tract (CIIT 1999). At low concentrations, inhaled FA is detoxified in the epithelial layers of nasal cavity. Free FA is conjugated to glutathione by glutathione *S*-transferase, thus forming the conjugate *S*-hydroxymethylglutathione (Figure 3). Subsequently, FA dehydrogenase oxidizes *S*-hydroxymethylglutathione to *S*-formylglutathione, which is further hydrolyzed to formate and glutathione (Heck *et al.* 1988). Formate is either excreted with the urine or dehydrogenated to carbon dioxide being exhaled (Oro *et al*. 1959).

Cells treated with low FA doses (100 nM) respond with enhanced cell proliferation and decreased apoptosis (Marcsek *et al*. 2007) whereas, at higher concentrations (>10 µM), FA inhibits cell proliferation and promotes apoptosis (Tyihak *et al*. 2001). These apparently contradicting effects suggest that FA becomes cytotoxic upon saturation of the glutathione system.

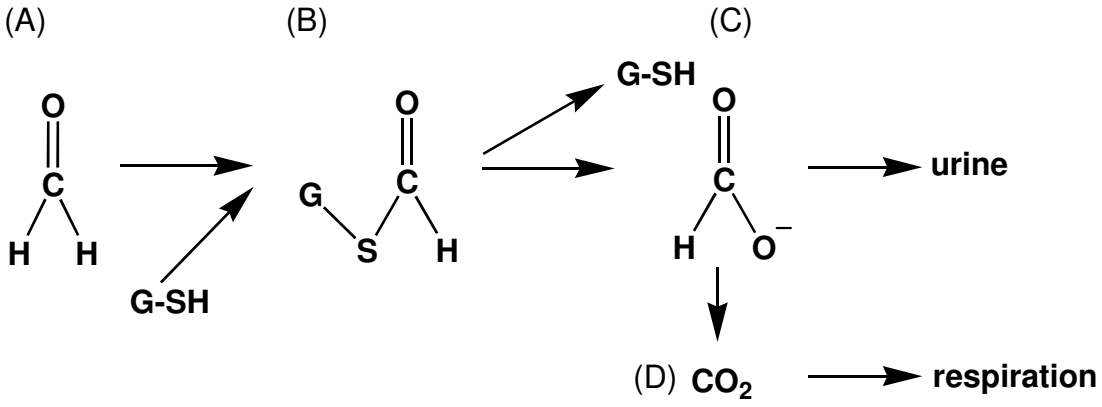

Figure 3: *Metabolism of FA. (A) Conjugation with glutathione (G-SH), leading to the formation of S-formylglutathione. (B) S-formylglutathione is then hydrolyzed to glutathione and formate. (C) Formate is either excreted in the urine (D) or is further metabolized to water and carbon dioxide, which is exhaled.*

Free reactive FA is genotoxic as it generates DNA-protein crosslinks (DPXs), induces sister chromatid exchanges and micronuclei (Heck & Keller 1988; Hubal *et al*. 1997; Merk & Speit 1998). The primary mutagenic effect of FA is attributed to the formation of DPXs (Casanova *et al*. 1991; Conaway *et al*. 1996), whereby a DNA-binding protein is covalently linked to the amino group of a DNA base (Figure 4). Studies performed in rats and monkeys indicate that DPX formation is proportional to the tissue FA concentration (Casanova *et al.* 1991, 1994). A fraction of these DPXs are reverted by hydrolysis combined with proteolytic degradation (Quievryn & Zhitkovich 2000). However, there is very limited information of the repair of DPXs besides their spontaneous removal. Some biochemical studies suggest that the NER system is involved in the elimination of DPXs (Minko *et al*. 2002; Reardon *et al*. 2006).

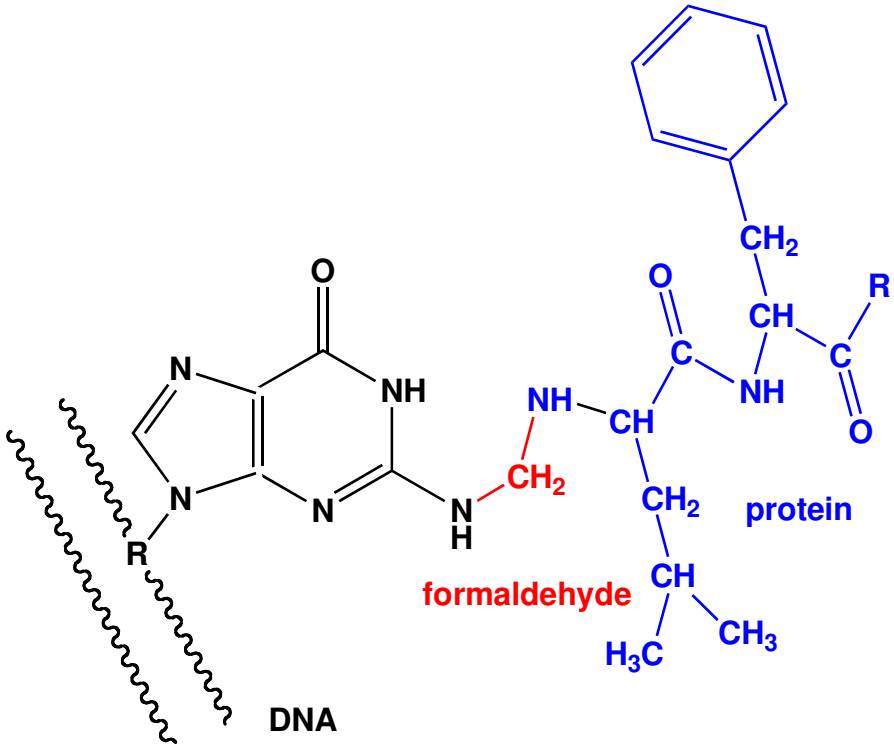

Figure 4: *Basic structure of a DNA-protein crosslink induced by FA exposure.*

3 AIMS OF THE THESIS

The primary aim of this work was to establish a live-cell imaging system based on differentially fluorescent protein tags to study the dynamic trafficking of DNA damage recognition factors (primarily XPC and DDB) involved in the human NER pathway. The second aim was to validate this live-cell imaging system by monitoring the response of DNA damage recognition factors to standard genotoxic stress induced by exposure to UV radiation or treatment with the alkylating agent cisplatin. The third goal was to apply the live-cell imaging system to test how XPC and DDB respond to FA-induced DPXs.

4 MATERIALS AND METHODS

4.1 Cell culture

Simian virus 40-transformed human XP-C fibroblasts (GM16093) and wild-type fibroblasts (GM00637) were purchased from Coriell Cell Repository (Camden, New Jersey, USA). These fibroblasts were cultured in Dulbecco's Modified Eagle Medium (DMEM; Gibco) containing 10% fetal bovine serum (FBS; Gibco), 0.1 U/ml penicillin and 0.1 µg/ml streptomycin (Gibco). All cells were incubated at 37℃ in a humidified atmosphere containing 5% CO_2.

4.2 Mammalian expression vector and cloning

The complementary DNA coding for human DDB2, XPC, XPA and XPD were fused to the sequence of various fluorescence proteins using the restriction enzymes (New England BioLabs) listed in Table 1. Vectors containing the sequence of fluorescent proteins (pEGFP, pECFP, pEYFP) were ordered from Clontech. The pmRFP1 - C3 was kindly provided by Dr. Elisa May (University of Konstanz, Germany); pEGFP–DDB2-C1 was a gift from Dr. Stuart Linn (University of California, Berkeley, USA) and XPD-pEGFP-N1 from Jean-Marc Egly (University Louis Pasteur, Strasbourg, France). The plasmid pEGFP-Ub-C1 was purchased from the non-profit organization Addgene (www.addgene.org).

Table 1: *Plasmids and restriction enzymes used in the course of this thesis*

Protein	Original plasmid	Target vector	Restriction enzymes
DDB2	pEGFP-DDB2-C1	pmRFP1- C3	*BamH*1
DDB2	pEGFP-DDB2-C1	pECFP-C1	*BamH*1
DDB2	pEGFP-DDB2-C1	pEYFP-C1	*BamH*1
XPC	XPC-pcDNA	pEGFP-N3	*Kpn*1, *Xma*1
XPC	XPC-pEGFP-N3	pmRFP1-C3	*Kpn*1, *Sma*1
XPC	XPC-pEGFP-N3	pECFP-C1	*Kpn*1, *Sma*1
XPC	XPC-pEGFP-N3	pEYFP-C1	*Kpn*1, *Sma*1
XPD	XPD-pEGFP-N1	pmRFP1-C3	*Kpn*1, *EcoR*1

The expression vectors were constructed basically following the methods described by Sambrook *et al.* (1989). Each plasmid was digested for 2 h using the appropriate restriction buffers (New England BioLabs) and enzymes as indicated in Table 1. To avoid self-ligation, vectors treated with enzymes generating blunt ends were dephosphorylated using calf intestine alkaline phosphatase (CIP; New England BioLabs) for 1 h at 37℃. Digestion mixtures were loaded on a 1% agarose gel for purification. The fragment coding for the proteins of interest (insert) and the linearized acceptor vector were extracted using QIAquick Gel Extraction Kit (QIAGEN) or Geneclean Turbo Kit (Q-BIOgene). Subsequently, 90 fmol of the insert and 30 fmol of the linearized vector were ligated by T4 DNA ligase (Promega) in overnight incubations at 16℃ or for 4-h incubations at 25℃. If necessary, site-directed mutagenesis (QuickChange II Site-Directed Mutagenesis Kit; Stratagene) was used to correct the frame or to insert a STOP codon. The respective oligonucleotide primers are listed in Table 2. All final clones were sequenced (Microsynth) to exclude accidental mutations introduced elsewhere in the complementary DNA.

Table 2: *PCR primers used for site-directed mutagenesis*

Plasmid	Oligonucleotide sequences
pmRFP1-DDB2	Insertion primers 5'-CTCCACCGGCGCCACTGTACAAGTACTC-3' 5'-GAGTACTTGTACAGTGGCGCCGGTGGAG-3'
pmRFP1-XPC	Stop primers 5'-CATTTGAGAAGCTGTGACCCGGGATCCACC-3' 5'-GGTGGATCCCGGGTCACAGCTTCTCAAATG-3'
pmRFP1-XPD	Insertion primers 5'-CTCCACCGGCGCCACTGTACAAGTACTC-3' 5'-GAGTACTTGTACAGTGGCGCCGGTGGAG-3'

4.3 Induction of local DNA damage and immunochemistry

One day before transfection, 400'000 cells were seeded into 6-well plates containing glass cover slips. At a confluence of 90%, the cells were transfected with 1 µg DNA using 4 µl FuGENE HD transfection reagent (Roche). For co-transfections, 0.75 µg of each plasmid and 6 µl transfection reagent were used. After 4-h incubations, the transfection mixture was replaced by complete medium and the cells were grown for another 18 h at 37°C.

Following removal of the cell culture medium and rinsing with phosphate-buffered saline (PBS), the cells were irradiated through 5-µm diameter pores of a polycarbonate filter (Millipore) using a UV source (254 nm, 150 J/m^2) at a dose rate of 3 W/m^2. Thereafter, cells were incubated in complete DMEM for 10 min at 37°C. Subsequently, the cells were washed with PBS and fixed with 4% paraformaldehyde in PBS for 15 min at room temperature. After washing in PBS, the cells were permeabilized five times with 0.1% TWEEN 20 in PBS and the DNA was denatured with 0.07 M NaOH in PBS for 8 min. The cells were washed five times with 0.1% TWEEN 20 in PBS and treated with 20% FCS in PBS for 30 min at 37°C to inhibit unspecific binding. Subsequently, the cells were incubated (1 h, 37°C) with the primary antibody directed against CPDs (TDM-2, MBL International Corporation), diluted 1:3000 with 5% FCS in PBS. After incubation with the primary antibody, cells

were washed five times with 0.1% TWEEN 20 in PBS and blocked twice with 20% FCS in PBS for 10 min. Samples were treated with the appropriate Alexa Fluor dye-conjugated secondary antibody (Invitrogen; dilution 1:400) and incubated for 30 min at 37° C. Finally, the cells were washed five times with 0.1% TWEEN 20 in PBS and the nuclei were stained with HOECHST 33342 (Invitrogen; 200 ng/ml) for 10 min. The samples were finally washed three times with PBS and fixed on an objective slide using Fluoromount G (Interchim). These samples were analyzed through a 60x oil immersion objective using a Leica TCS SP5 confocal microscope to quantify both the green fluorescence of the transfected fusion protein and the red fluorescence representing UV lesions detected by monoclonal antibodies.

4.4 Host cell reactivation assay

This DNA repair assay is based on the *in vivo* removal of DNA lesions from an irradiated expression vector coding for the *Photinus* (firefly) luciferase enzyme. The results are normalized for transfection efficiency by concomitant co-expression of the *Renilla* luciferase from an undamaged vector. For that purpose, 400'000 human fibroblasts were seeded in 6-well plates. The next day, at a confluence of 90%, samples were transfected in triplicates with 0.5 µg plasmid DNA and 0.5 µg luciferase mixture containing UV irradiated (1000 J/m^2) pGL3 (coding for *Photinus* luciferase) and phRL-TK (unirradiated, coding for *Renilla* luciferase) in a ratio of 10:1. The FuGENE HD reagent (Roche) was used for transfection, which was carried out in complete medium supplemented with FA (Fluka) as indicated. After 4 h at 37°C, the transfection mixture was replaced by complete cell culture medium and the fibroblasts were incubated for another 18 h. Subsequently, the cells were lysed in 500 µl 5x Passive Lysis Buffer (Promega) following the manufacturer's instructions. The lysates were cleared by centrifugation and, subsequently, the expression of *Photinus* and *Renilla* luciferase activity was determined using the Dual-Luciferase reporter assay system (Promega). The luminescent signal from the luciferase reaction was monitored in a MLX microplate luminometer (Dynex). All results were normalized by calculating the ratios between *Photinus* luciferase activity and the internal *Renilla* standard.

4.5 Fluorescence recovery after photo bleaching

Cells were grown for 24 h on cover slips and transfected with vectors coding for fluorescence-tagged repair factors using the FuGENE HD reagent. After 4 h at 37℃, the transfection mixture was replaced with complete medium and incubated for another 18 h. To measure the influence of UV light, formaldehyde or cisplatin on protein mobility, fluorescence recovery after photobleaching (FRAP) experiments were performed with a 63x oil immersion objective using a Leica TCS SP5 confocal microscope. During the FRAP experiment, cells were kept at 37℃ and 5% CO_2 in a climate chamber. The nuclear fluorescence within the region of interest (ROI) was photobleached for 2.2 sec at 100% intensity with a 488 nm Argon ion laser. To increase the bleaching efficiency, a 405 nm UV laser in addition to the argon ion laser was used for GFP-DDB2, GFP-OGG1 and their mutants. Before and after bleaching, confocal image series were recorded at 120-ms time intervals (typically 75 prebleach and 200 postbleach frames) at low laser intensity. Simultaneously, a reference ROI of the same size was measured for each time point. Confocal image series were recorded with a frame size of 128 × 128 pixels and a scanner frequency of 1400 Hz. Mean fluorescence intensities of the bleached region were corrected with the reference ROI and normalized to the mean of the last 30 prebleach values.

4.6 Treatments with DNA damaging agents

To study the response of the DNA damage recognition factors to genotoxic stress, cells were exposed either to FA (Fluka), cisplatin (Sigma-Aldrich) or UV irradiation. Four h after transfection, the transfection mixture was replaced by complete medium supplemented with formaldehyde (0 µM – 100 µM) or cisplatin (5 µM) and cells were incubated for another 16 hours. For FRAP experiments in cells exposed to UV-irradation, the tranfection mixture was replaced by complete medium and incubated for another 16-20 h, followed by irradiation with a dose of 10 J/m2 using a UV-C source (254 nm wavelength).

5 RESULTS

5.1 Production of fluorescent fusion proteins

To analyze the DNA repair processes of living cells in real-time, several subunits of the nucleotide excision repair (NER) pathway were tagged with enhanced cyan, enhanced green, monomeric red or enhanced yellow fluorescent proteins (ECFP, EGFP, mRFP, EYFP) as summarized in Table 3. For that purpose, appropriate molecular cloning was performed to introduce the complementary DNA of interest into a final vector carrying the sequence for one of the fluorescent tags (see Material & Methods). One of these vectors also codes for a GFP-tagged ubiquitin moiety (pEGFP-Ub-C1) that has been purchased from a commercial source to monitor DNA damage-induced ubiquitylation reactions.

Table 3: *Overview of fluorescent constructs. The letters N and C describe the position of the gene of interest relative to the fluorescent protein (N, amino-terminal; C, carboxy-terminal).*

Color	XPC	DDB2	XPD	Ubiquitin
green	XPC-pEGFP-N3	pEGFP-DDB2-C1	XPD-pEGFP-N1	pEGFP-Ub-C1
red	pmRFP1-XPC-C3	pmRFP1-DDB2-C3	pmRFP1-XPD-C3	
cyan	pECFP-XPC-C1	pECFP-DDB2-C1		
yellow	pEYFP-XPC-C1	pEYFP-DDB2-C1		

All constructs were sequenced to exclude accidental mutations in the complementary DNA and, subsequently, transfected into mammalian cells to monitor overall expression levels and sub-cellular distributions. As expected, the DNA damage recognition subunits XPC (Figure 5) and DDB2 (data not shown) display a clear nuclear localization regardless of the color of the fluorescent tag.

A different distribution was observed for XPD protein, which appears mainly localized to the cytoplasm (Figure 6). This finding suggests that the fluorescently tagged XPD fusions were not correctly incorporated into the 10-subunit transcription factor TFIIH

complex (Santagati *et al*. 2001) or, alternatively, that the tagged XPD was produced in vast excess in comparison to the other TFIIH subunits. As a consequence, no further studies have been conducted with the XPD fusion products.

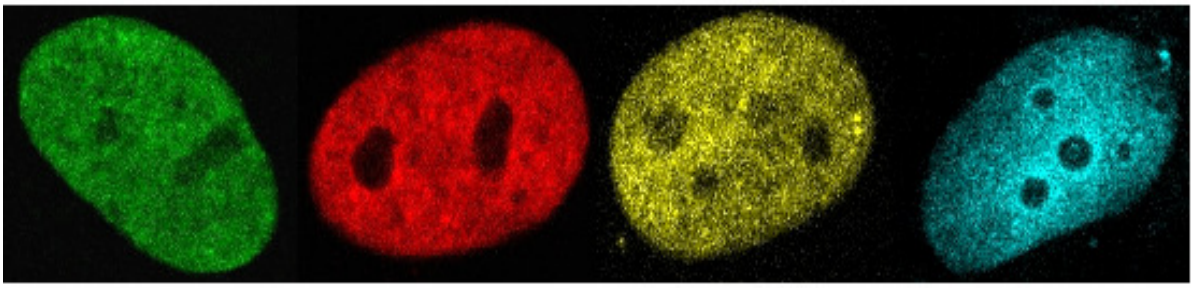

green red yellow cyan

Figure 5*: Nuclear localization of XPC tagged with the different fluorescent proteins encoded by XPC-pEGFP (green), pmRFP1-XPC (red), pEYFP-XPC (yellow) and pECFP-XPC (cyan).*

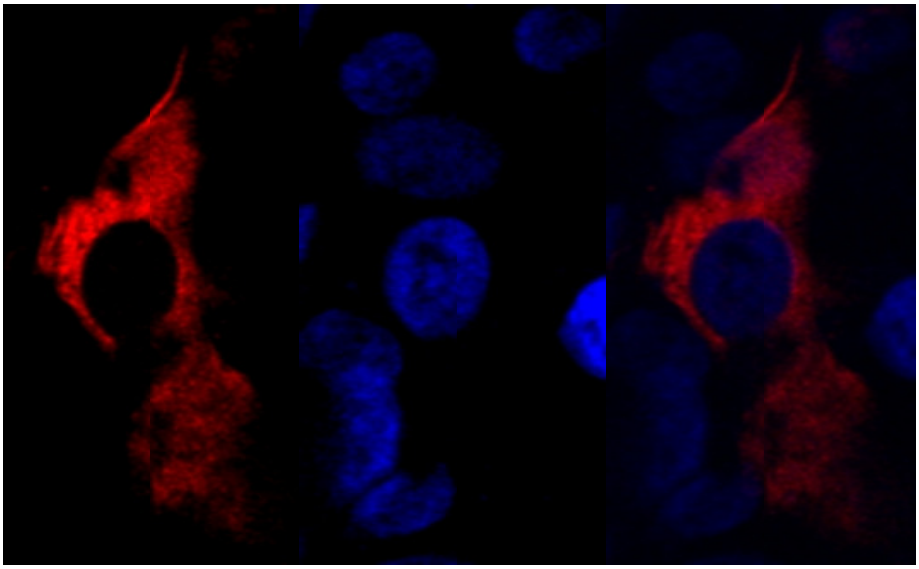

pmRFP1-XPD Hoechst merge

Figure 6*: pmRFP1-XPD is mainly localized to the cytoplasm. Hoechst, DNA staining to visualize the nucleus.*

Finally, the N-terminal GFP-tagged ubiquitin, which remains active as shown elsewhere (Dantuma *et al*. 2006), is mainly detected in the nucleus although it is found to a lower extent in the cytoplasm as well.

5.2 Functionality of the fusion proteins

The fusion proteins were examined in terms of their functionality by two different methods. An overall repair activity was determined by monitoring excision activity in a host-cell reactivation assay. Second, the damaged DNA-binding activity was measured by monitoring the capacity of each fusion product to accumulate at foci of DNA damage induced by UV irradiation through the pores of polycarbonate filters.

5.2.1 Repair proficiency in the host-cell reactivation assay

To test whether any of the introduced fluorescent tags affect the repair activity, the constructs were compared in a host-cell reactivation assay that has been developed to measure NER activity in living cells (Carreau *et al*. 1995). NER-deficient XP-C fibroblasts were transfected with a dual luciferase reporter system accompanied by an expression vector coding for the XPC protein to restore the repair activity of the cell line. One of the reporter plasmids (pGL3) contains the UV-irradiated complementary DNA coding for firefly luciferase. The second plasmid (phRL-TK), carrying the non-irradiated *Renilla* luciferase gene, is needed to normalize the values for transfection efficiency. After 18-h incubations, the firefly luciferase activity in cell lysates was measured in a luminometer, followed by normalization against the *Renilla* luciferase control. We found that all XPC fusion proteins corrected the repair defect of XP-C cells. In fact, the human fibroblasts expressing pECFP-XPC, pEYFP-XPC or pXPC-EGFP (thereafter referred as XPC-GFP) display essentially the same repair activity as those containing the non-tagged version of XPC protein (expressed from pcDNA-XPC), indicating that the fusion of this particular NER factor to a fluorescent partner does not interfere with its physiological function in DNA repair. As a control, we demonstrated that the excision repair activity was not rescued when the cells were transfected with the empty pcDNA vector (Figure 7).

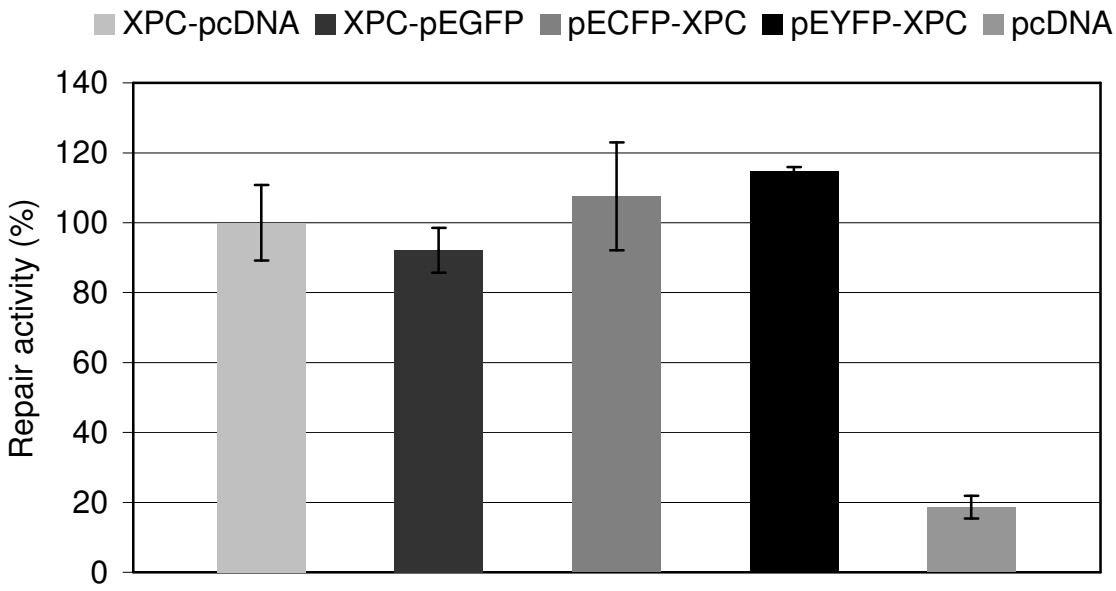

***Figure 7**: Host-cell reactivation assay measuring the repair activity in living cells. DNA repair is indicated as the percentage of luciferase gene reactivation after transfection of XP-C fibroblasts with vectors coding for full-length XPC protein alone or in conjugation with a fluorescent partner. The luciferase activity observed with full-length XPC was taken as the reference value and set to 100%; pcDNA, empty expression vector resulting in background host-cell reactivation levels. Error bars represent standard deviations (n = 3).*

5.2.2 DNA damage recognition proficiency

The fluorescently tagged repair proteins were also analyzed for their relocalization to repair foci induced by irradiation with UV-C light (254 nm wavelength). Human NER-proficient fibroblasts were grown on cover slips and transfected with plasmids coding for the different fluorescent fusion products. Subsequently, the cells were UV-irradiated through the pores of polycarbonate filters, thereby generating foci of DNA damage. This exposure to UV light results in the formation of two major classes of photoproducts, i.e., cyclobutane pyrimidine dimers (CPDs) and pyrimidine (6-4) pyrimidone photoproducts (Pfeifer 1997). Both type of damages are efficiently recognized and repaired by the NER pathway, thus leading to a local accumulation of the repair proteins at lesion sites. The detection of CPDs with specific antibodies,

following fixation of the cells, was used to confirm that the assembly of NER complexes took place at sites of DNA damage. We found that all fusion proteins with XPC and DDB2, listed in Table 3, efficiently accumulate at these repair foci. Figure 8 illustrates the co-localization of pEGFP tagged DDB2 (thereafter referred as GFP-DDB2) with foci of UV lesions in the nuclei of human fibroblasts.

(A) (B)

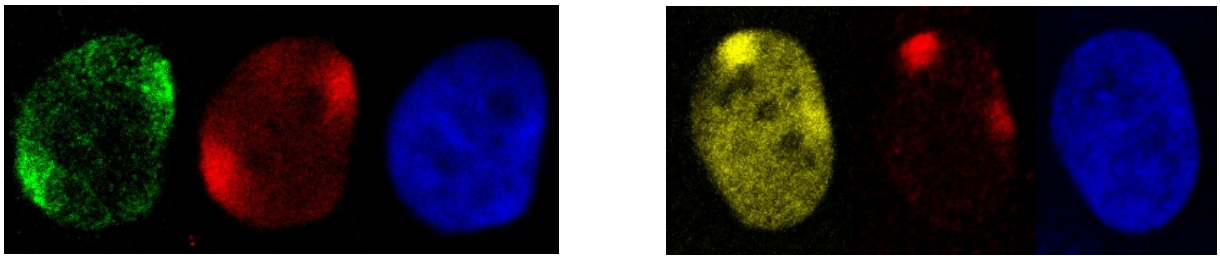

GFP-DDB2 CPDs Hoechst YFP-DDB2 CPDs Hoechst

Figure 8*: Expression of GFP-DDB2 (A) and YFP-DDB2 (B) in repair-proficient human fibroblasts. The cells were irradiated with UV-C light (150 J/m^2) through the 5-µm pores of polycarbonate filters and subjected to fixation 15 min after this treatment. The formation of CPDs was demonstrated by immunochemical staining with the red dye Alexa 546. Nuclei were stained using Hoechst dye, which visualizes the cellular DNA (blue).*

5.3 Live cell imaging

Live cell imaging using fluorescently labeled proteins provides several innovative opportunities to monitor the dynamics of individual repair factors as well as the assembly and disassembly of multi-subunit repair complexes within the physiologic microenvironment of living cells. Fluorescence recovery after photobleaching (FRAP), for instance, is already widely applied in many fields to determine the dynamics of GFP-tagged proteins in living cells. In this study, FRAP was employed to study the changes in the mobility of repair proteins when cells are exposed to genotoxic stress. For that purpose, the fluorescent tag of the fusion protein is bleached across a defined area of the nucleus. Thereafter, the recovery of the fluorescence signal within the bleached area is monitored over time to assess DNA damage-induced

differences in protein mobility, which are indicative of the engagement of a particular factor with DNA damage responses.

5.3.1 Processing of FRAP data

The fluorescence signal of GFP-tagged proteins was detected through a confocal laser scanning microscope by measuring average pixel values in defined regions of interest (ROI 1) within the nuclear compartment. An image of each cell comprising the ROI 1 was collected before bleaching and at several time points during the subsequence fluorescence recovery. Simultaneously, a reference ROI (ROI 2) of the same size was taken for each time point in a neighboring area of the same nucleus. Representative data sets obtained from three human fibroblasts are displayed in Table 4.

***Table 4**: Example of raw data generated during the first three seconds of typical FRAP experiments with GFP-tagged NER factors.*

Fibroblast 1			Fibroblast 2			Fibroblast 3		
Time	ROI 1	ROI 2	Time	ROI 1	ROI 2	Time	ROI 1	ROI 2
0	57365,73	56169,96	0	35969,83	37139,01	0	44765,48	42778,68
0,11	57406,01	55031,26	0,12	36150,12	37234,79	0,11	44375,8	42433,66
0,23	57819,33	55542,75	0,24	35538,16	37442,36	0,23	44322,45	42583,57
0,35	56798,87	55685,71	0,36	35211,04	36342,04	0,35	43864,89	42230,04
0,46	57339,97	54942,32	0,47	36221,41	36259,82	0,46	44089,14	43154,39
0,57	56965,47	54247	0,58	35319,37	36156,63	0,57	43848,82	42757,1
0,69	56591,24	54491,97	0,7	35436,32	36672,25	0,69	43780,25	42620,19
0,8	56921,09	55217,46	0,81	35077,65	36242,09	0,8	44186,07	42464,79
0,91	56829,88	55187,1	0,93	35868,76	35690,51	0,91	44418,51	42258,67
1,03	56564,04	55382,44	1,04	34662,02	35895,57	1,03	44111,12	42250,83
1,15	56570,92	55112,12	1,16	34876,13	36253,6	1,15	44132,02	41346,89
1,26	57145,74	55679,75	1,27	35376,61	35648,91	1,26	43704,47	42647,46
1,38	56656	55256,41	1,39	35459,93	36232,5	1,38	43920,58	42500,04
1,49	56881,53	54685,27	1,5	35250,07	36177,65	1,49	44335,96	42240,63

1,61	56161,18	54432,07	1,62	34962,57	36538,75	1,61	43887,62	42377,35
1,72	56494,39	54089,83	1,74	35649,76	36144,2	1,72	43927,28	42372,5
1,84	56412	54870,54	1,85	35293,3	35949,66	1,84	44051,95	41753,98
1,95	56591,28	54700,04	1,97	34827,99	36360,46	1,95	42459,67	41609,39
2,07	56544,07	54745,68	2,08	35867,58	36462,53	2,07	43795,64	42383,81
2,18	56320,06	54388,54	2,19	34674,13	36216,3	2,18	44363,96	42011,45
2,3	56214,55	54606,97	2,31	35635,93	36421,61	2,3	43262,43	42577,6
2,41	56097,07	54653,34	2,42	34580,13	35721,57	2,41	43190,21	41548,96
2,52	56238,58	54123,91	2,54	36142,89	36037,02	2,52	43658,67	42064,88
2,64	56352,47	54591,12	2,65	34574,8	36378,13	2,64	43349,82	42036,88
2,75	56840,8	54720,38	2,77	35721,89	36667,23	2,75	43913,07	41425,04
2,88	56992,53	54523,96	2,89	35822,27	36880,4	2,88	43123,86	42125,76

In each single experiment, fluorescence recovery was monitored about 280 times translating to a total observation period of 30 seconds. Average values from at least 10 independent cells were used to determine the final fluorescence recovery plot. During the data analysis, the fluorescence signals were corrected for laser-induced fluctuations by dividing the intensities of ROI 1 by those in ROI 2 at each time point. Subsequently, all data were normalized to the pre-bleach intensities (Figure 9).

$$\text{Fluorescence signal} = \frac{\text{ROI 1}(t)}{\text{ROI 2 }(t)} \times \frac{\text{ROI 2 }_{(t5,4sec\text{-}8,5sec)}}{\text{ROI 1}_{(t5,4sec\text{-}8,5sec)}}$$

Figure 9*: Equation used for normalization and correction of laser intensity and photobleaching signals in FRAP experiments.*

5.3.2 Comparison of EGFP mobility by FRAP analysis

In a first series of experiments, FRAP was applied to cells expressing GFP without any fusion partner. As shown in Figure 10, the GFP moiety exhibits a very fast and complete recovery after photobleaching, indicating that GFP itself diffuses freely in the cell and does not bind to DNA or any other macromolecular structure. From these findings it can be concluded that the GFP tag does not disturb the mobility of repair proteins through unspecific interactions with nuclear constituents (Houtsmuller *et al*. 1999; Rademakers *et al*. 2003; Luijsterburg *et al*. 2007).

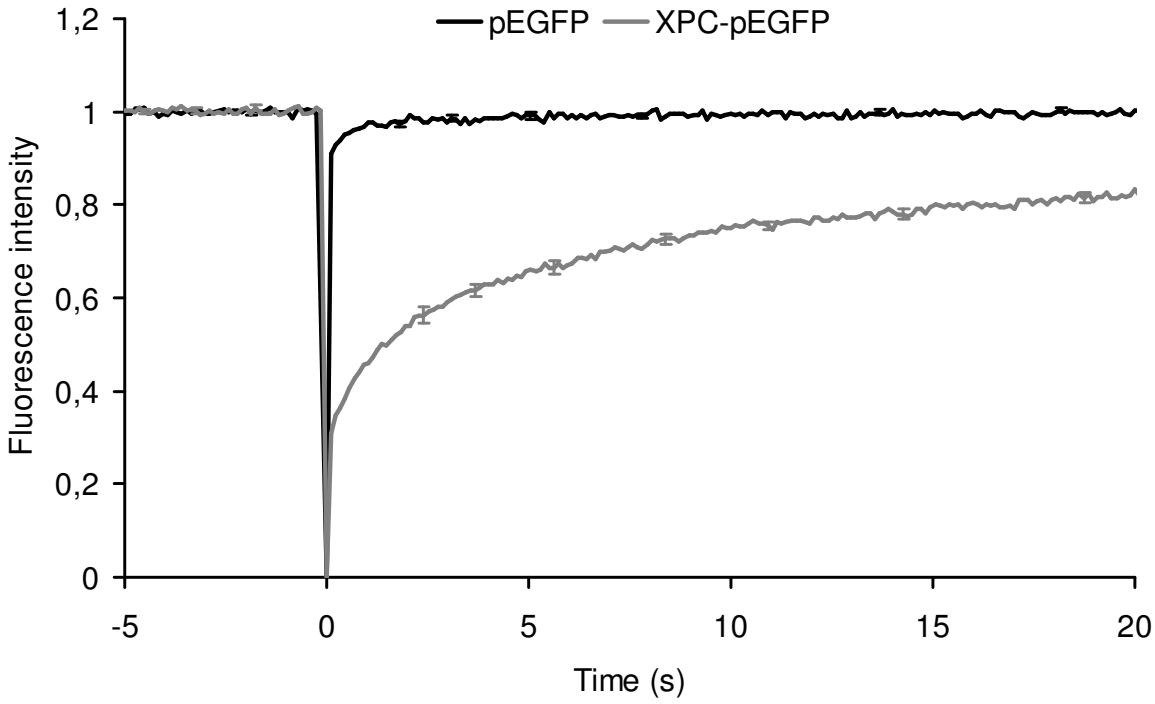

Figure 10*: Mobility of pEGFP moieties within the physiologic nuclear environment of living human fibroblasts. A defined nuclear area was bleached with a 488-nm laser and monitored at regular intervals of 120 milliseconds. The upper (bold) line shows the fluorescence recovery with the GFP polypeptide alone. The lower (grey) line reflects the mobility of the* **XPC-GFP** *fusion product in undamaged cells (n = 10; error bars represent standard errors of the mean).*

The overall fluorescence recovery was clearly retarded when the small GFP moiety was linked to the DNA damage recognition factor XPC (Figure 10). This substantial change in the diffusion rate cannot be explained solely by the increased size of the

fusion product (Hoogstraten *et al*. 2008) but rather indicates that the majority of XPC molecules bind constitutively to nuclear macromolecules such as DNA, thereby reducing its mobility. A similar effect can be observed when GFP is linked to the DNA damage recognition factor DDB2 (Figure 11).

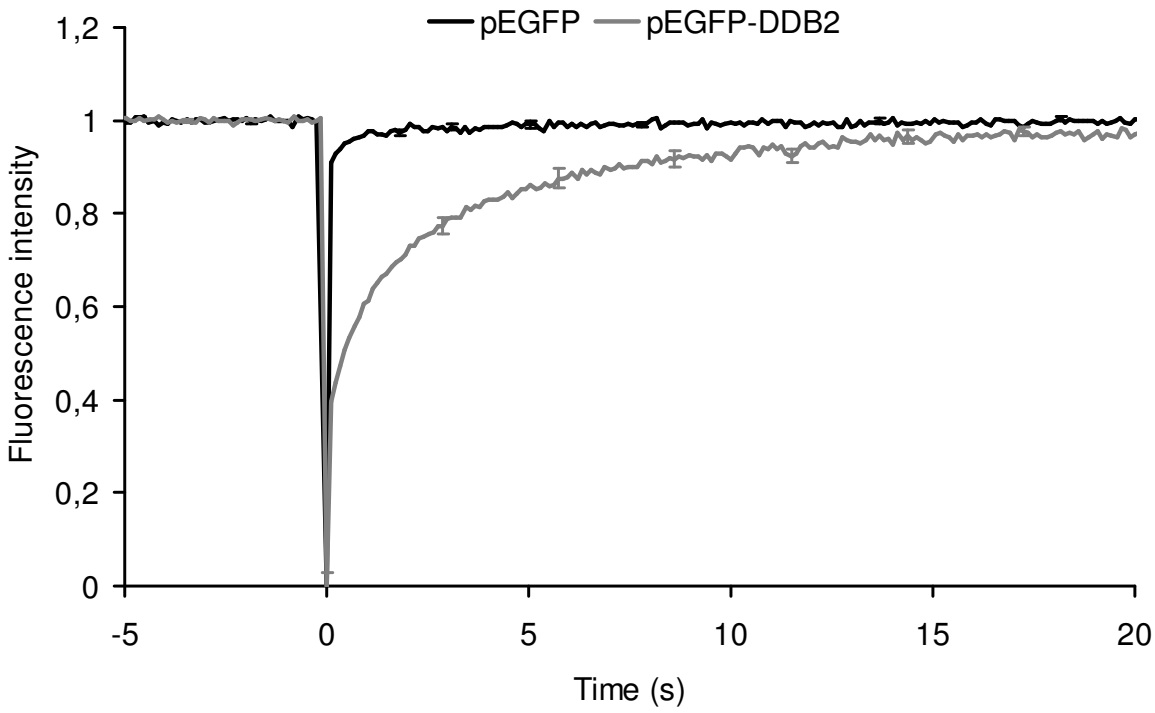

Figure 11*: Mobility of GFP moieties within the physiologic nuclear environment of living human fibroblasts. A defined nuclear area was bleached with a 488-nm argon ion laser and monitored at regular intervals of 120 milliseconds. The upper (bold) line shows the recovery of* **GFP** *alone. The lower (grey) line reflects the mobility of the* **GFP-DDB2** *fusion product in undamaged cells (n = 10; error bars represent standard errors of the mean).*

5.4 Application of FRAP – Live cell imaging upon genotoxic stress

Next, the FRAP analysis was used to investigate the effect of distinctly different genotoxic insults on the dynamics of the two DNA damage recognition factors XPC and DDB2 tested as GFP fusion proteins. For that purpose, human fibroblasts were transfected with XPC-GFP or GFP-DDB2 and exposed either to UV light, cisplatin or formaldehyde.

5.4.1 Response to DNA lesions induced by UV light

The initial recognition step of UV radiation-induced DNA lesions is carried out by DDB2 and XPC (Venema *et al*. 1991; Hwang *et al*. 1999). When the protein movement was monitored before and after UV irradiation, both XPC and DDB2 displayed the expected retardation in nuclear mobility (Figure 12). In the case of XPC protein, the baseline recovery of fluorescence reached a plateau at about 90% of the pre-bleach value, indicating that a fraction of this repair subunit is continuously bound to chromatin even in the absence of exogenously induced DNA damage (Hoogstraten *et al*. 2008; Camenisch & Naegeli 2009). In any case, the increased proportion of DNA-bound DDB2 and XPC proteins when the cells are exposed to UV light (Figure 12) is consistent with their function in the recognition and repair of DNA photoproducts.

(A)

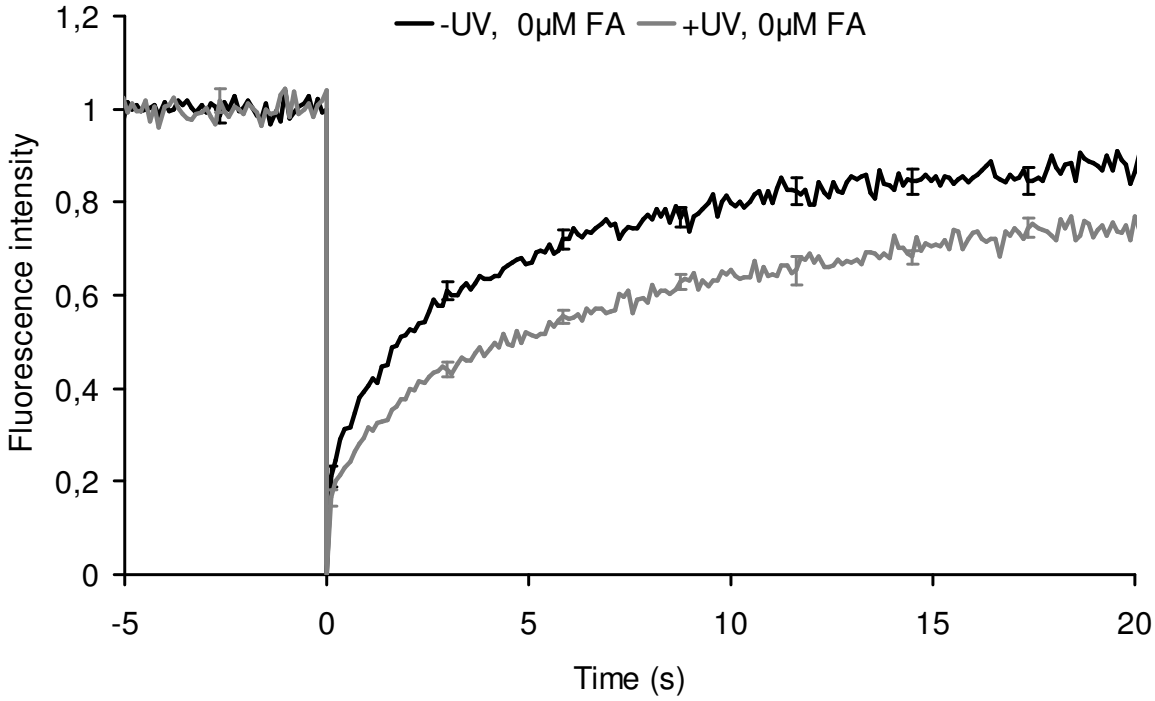

(B)

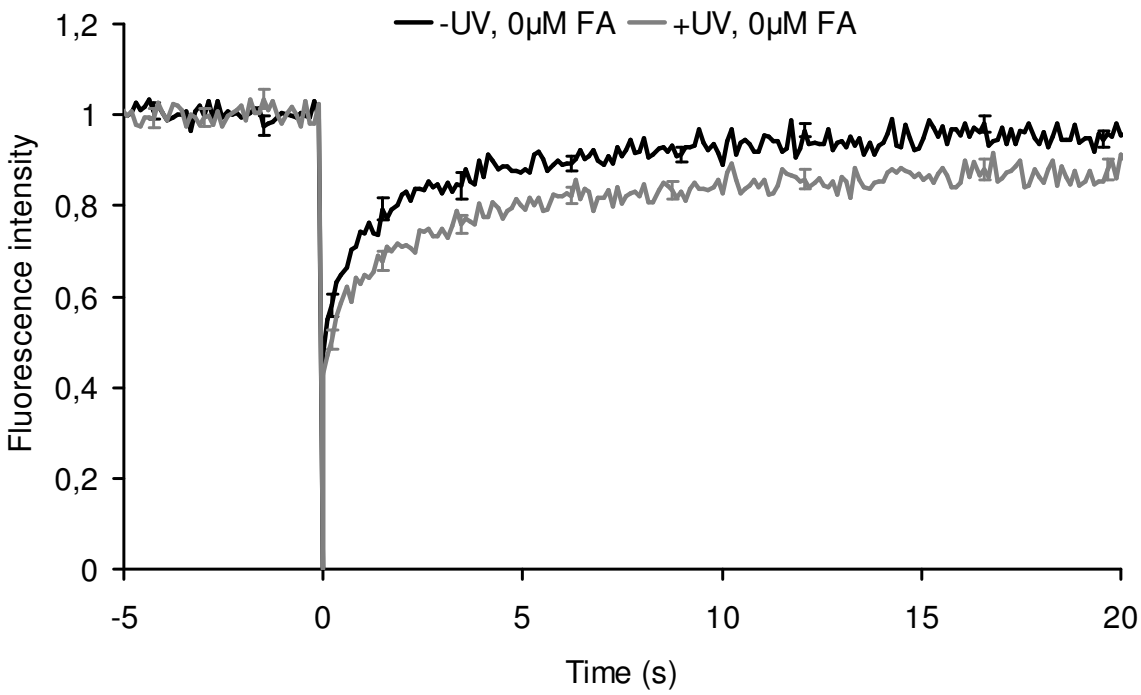

Figure 12: *Changes of FRAP kinetics of XPC-GFP and GFP-DDB2 following UV irradiation. Human XP-C fibroblasts were transfected with vectors* **XPC-pEGFP** *(A) or* **pEGFP-DDB2** *(B). Cells were irradiated with a UV-C dose of 10 J/m^2. The upper bold line represents the recovery of proteins in untreated cells. The lower grey curve shows the decreased mobility of the damage recognition factors in the presence of UV lesions (n = 10; error bars represent standard errors of the mean).*

5.4.2 Response to DNA lesions induced by cisplatin

It has been shown that cisplatin-induced DNA intrastrand crosslinks are removed by the NER pathway (Moggs *et al*. 1996; Furuta *et al*. 2002; Chen *et al*. 2003). Therefore, we tested the effect of a cisplatin treatment on the mobility of the initial recognition factors DDB2 and XPC in human fibroblasts. In both series of experiments, the exposure to cisplatin induced a moderate but significant reduction of the freely diffusing protein fraction, confirming the involvement of these NER subunits in the recognition of cisplatin-induced DNA lesions (Figure 13). In the case of DDB2,

we observed only a transient immobilization, suggesting that this particular subunit does not form stable interactions with cisplatin-damaged DNA.

***Figure 13**: Changes of FRAP kinetics of XPC-pEGFP and pEGFP-DDB2 following a cisplatin treatment. Human fibroblasts were transfected with* **XPC-pEGFP** *(A) or* **pEGFP-DDB2** *(B) and, for 16 h, exposed to cisplatin at a dose of 5 µM. The upper bold line represents the recovery of fluorescence in untreated cells. The lower grey curve reflects the decreased mobility of the damage recognition factors in the presence of cisplatin-DNA lesions (n = 10; error bars represent standard errors of the mean).*

(A)

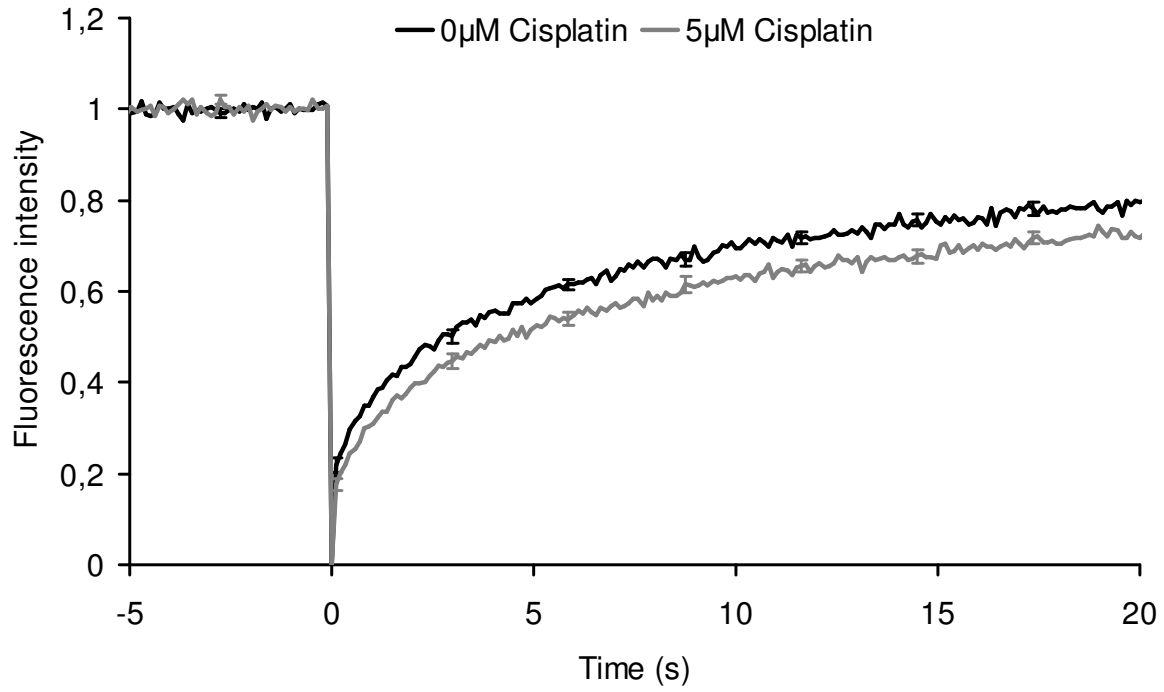

(B)

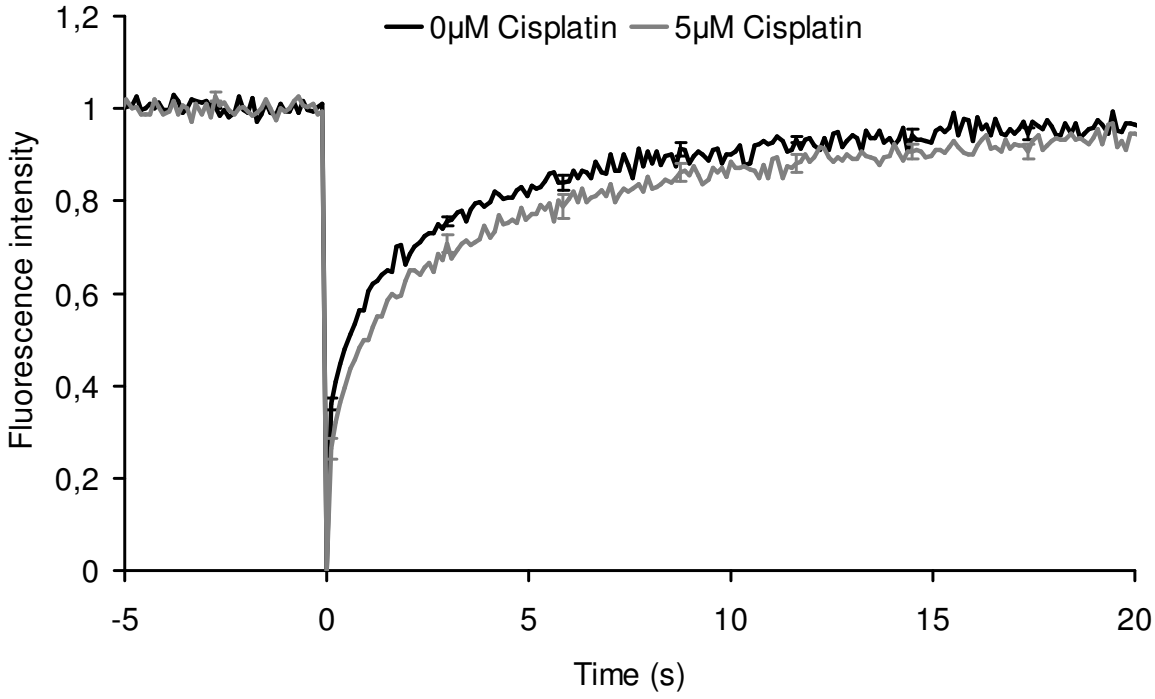

5.4.3 Response to DNA lesions induced by formaldehyde

Formaldehyde (FA) is another cross-linking agent that is able to damage the DNA double helix. In contrast to cisplatin, FA mainly induces the covalent binding of proteins to DNA, i.e. it forms DNA-protein crosslinks (DPXs) (Grafstrom *et al*. 1983; Merk & Speit 1998; Ridpath *et al*. 2007). Although it is unclear which DNA repair pathway is directly responsible for the removal of DPXs, recent reports suggest that the NER pathway may be involved in a final step during the processing of DPXs in mammalian cells (Minko *et al*. 2002; Reardon & Sancar, 2006). To test whether DPXs are recognized by the NER subunits DDB2 or XPC, human cells exposed to a non-cytotoxic FA concentration (75 µM) were subjected to FRAP analysis. Surprisingly, we found that the nuclear dynamics of GFP-DDB2 is significantly diminished by the low-dose FA treatment (Figure 14). In contrast, the mobility of XPC-GFP is not affected by this low-dose FA exposure (Figure 15). In co-transfection experiments, we further found that XPC protein is not significantly immobilized by FA-induced crosslinks even when its interaction partner DDB2 is simultaneously overexpressed (Figure 16).

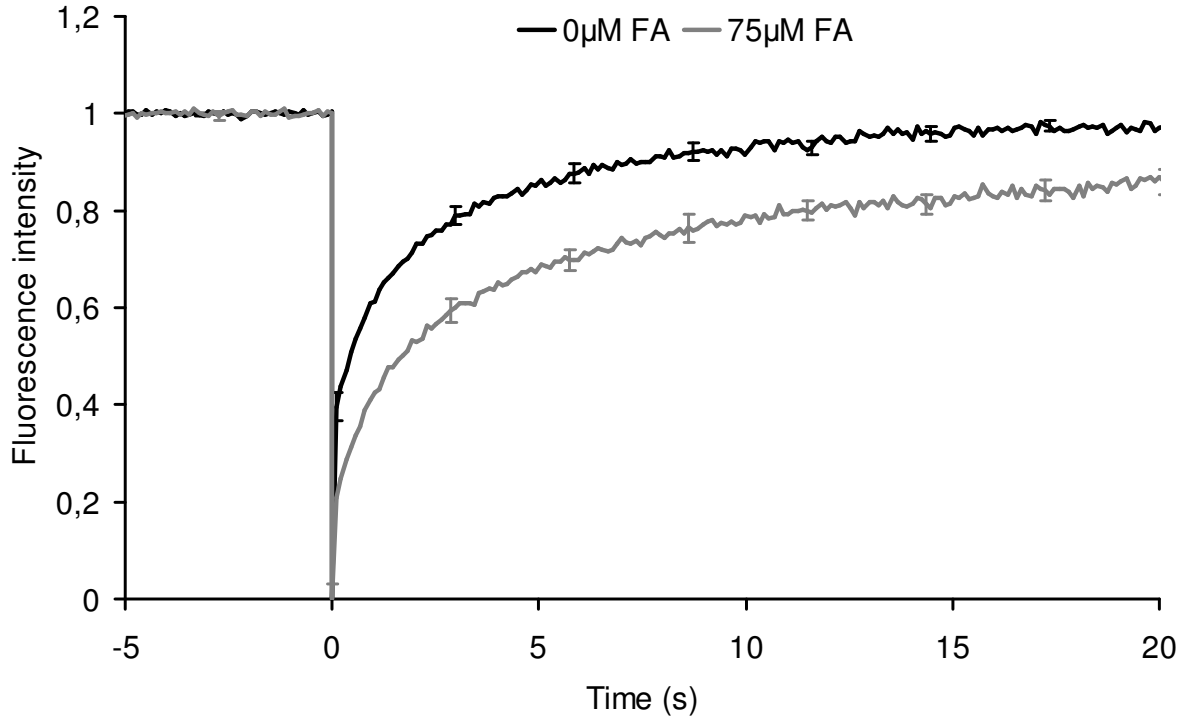

***Figure 14**: FRAP analysis of pEGFP-DDB2-transfected fibroblasts subsequently exposed for 16 h to a FA concentration of 75 µM. The upper bold line represents the fluorescence recovery of* **pEGFP-DDB2** *in untreated cells whereas the lower gray curve shows the decreased* **DDB2** *dynamics in FA-treated cells (n = 10; error bars represent standard errors of the mean).*

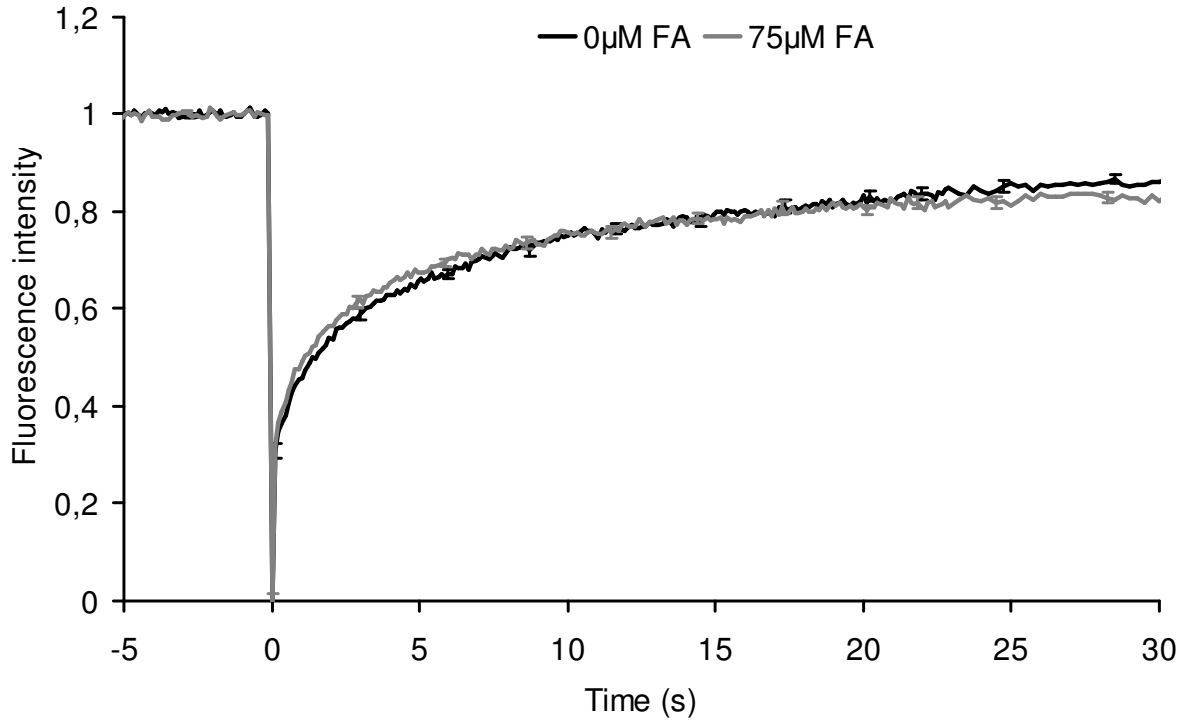

***Figure 15**: FRAP analysis of XPC-pEGFP-transfected fibroblasts subsequently exposed for 16 h to a FA concentration of 75 µM. The bold line represents the fluorescence recovery of* **XPC-pEGFP** *in untreated cells whereas the lighter gray curve shows that the* **XPC** *dynamics is not affected by the FA treatment (n = 10; error bars represent standard errors of the mean).*

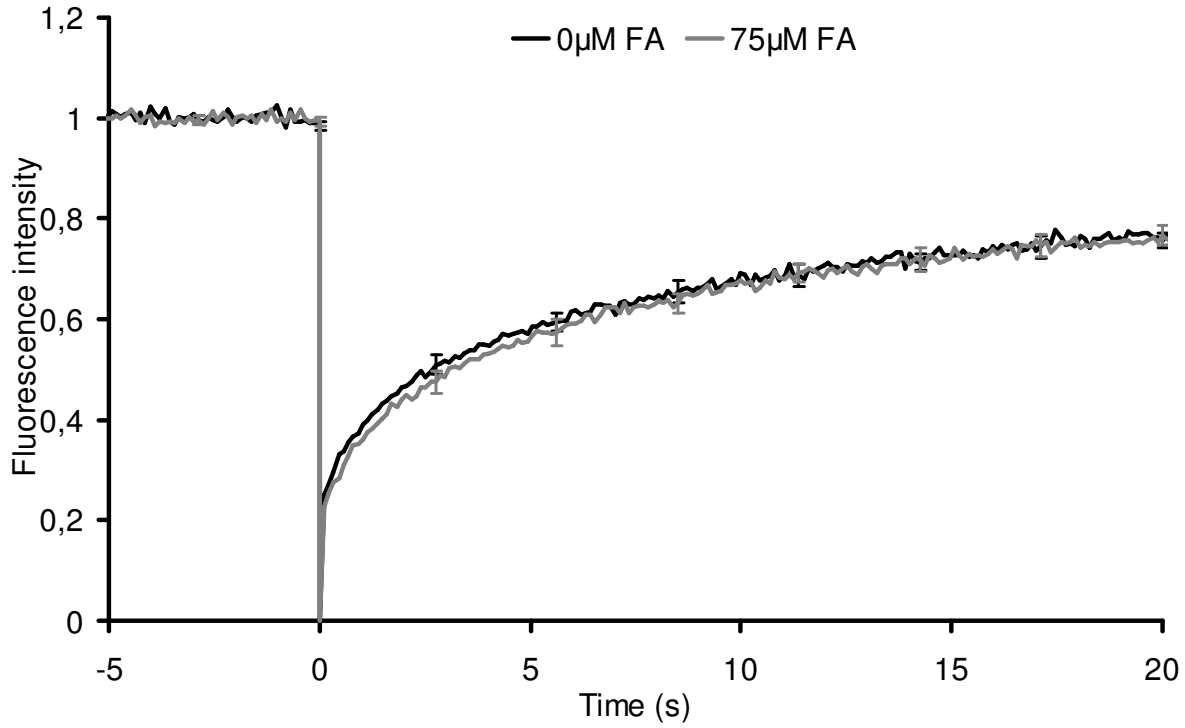

Figure 16**: Mobility of* **XPC-pEGFP**, *detected by FRAP, in human XP-C fibroblasts co-transfected with* **pmRFP1-DDB2** *and* **XPC-pEGFP** *and subsequently exposed for 16 h to a FA concentration of 75 µM. The bold line represents the fluorescence recovery of* **XPC-pEGFP** *in untreated* **mRFP-DDB2-expressing cells, whereas the gray curve shows the fluorescence recovery of* **XPC-GFP** *in the presence of* **mRFP-DDB2** *upon exposure to 75 µM FA (n = 10; error bars represent standard errors of the mean). See the following section for further details on the dual transfection with differentially fluorescent fusions.*

An important control experiment is to exclude that the GFP tag itself may be responsible in part for the changes of GFP-DDB2 dynamics observed in Figure 14 following FA treatments. For that purpose, FRAP analyses were performed in cells transfected with the empty vector pEGFP, by which the GFP moiety is expressed without any fusion partner. Figure 17 demonstrates that FA does not interfere with the very fast and complete recovery of fluorescence in these cells containing the free GFP moiety.

Taken together, our protein dynamics experiments indicate that the nuclear mobility of DDB2 but not XPC is retarded by exposure to a non-cytotoxic FA concentration. As DDB2 is generally thought to be specialized on the recognition of UV lesions, these

results suggest an unexpected involvement of this factor in processing or at least in the detection of FA-induced DPXs.

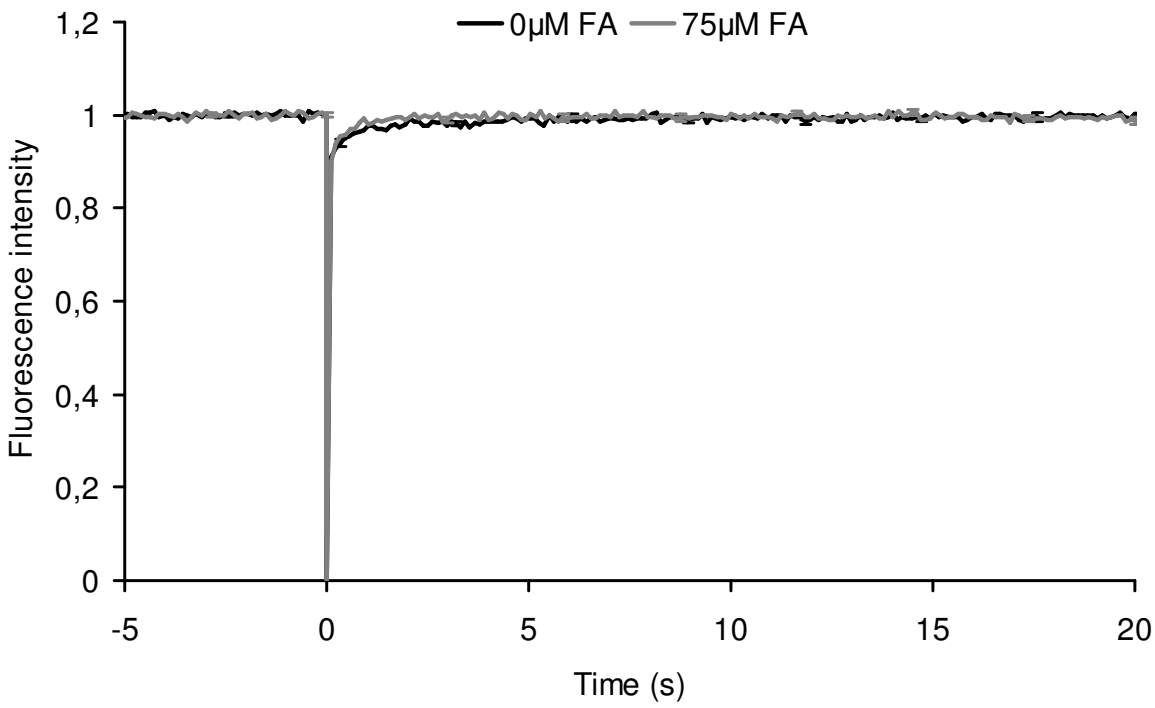

***Figure 17**: FRAP analysis plots demonstrating the rapid diffusion of GFP in both untreated (bold line) and FA-treated fibroblasts (gray line). The cells were transfected with* **pEGFP** *and exposed to 75 µM FA for 16 hours (n = 10; error bars represent standard errors of the mean). This control experiment shows that the rapid movement of GFP is not retarded by the FA treatment.*

5.5 Simultaneous expression of two tagged proteins

A principal goal of this thesis was to set up appropriate experimental conditions to monitor the cellular co-localization of different protein partners participating in the NER pathway. The wide repertoire of fluorescent tags (Table 3) allows for the simultaneous visualization of multiple proteins in living cells. Therefore, separate NER subunits were expressed in the same target cells as fusion proteins in association with differentially fluorescent partners.

5.5.1 Co-expression of fluorescent DDB2 and XPC proteins

The transfection procedure was adapted to express simultaneously two proteins in mammalian cells (for details see the Materials & Methods section). To exclude that co-transfections may interfere with the damage recognition function of XPC and DDB2 proteins, UV radiation foci were generated by irradiating the cells with UV-C light (150 J/m^2) through the pores of a Millipore filter. Subsequently, the localization of XPC-GFP and mRFP-DDB2 (co-expressed in the same cells) was monitored separately using the respective emission spectrum. Figure 18 demonstrates that XPC-GFP and mRFP-DDB2 accumulate simultaneously in the same DNA repair foci, implying that both proteins are functional and do not impede the accumulation of each other. The presence of UV lesions in these DNA repair foci was confirmed by immunochemical staining for CPDs with the blue dye Alexa 405.

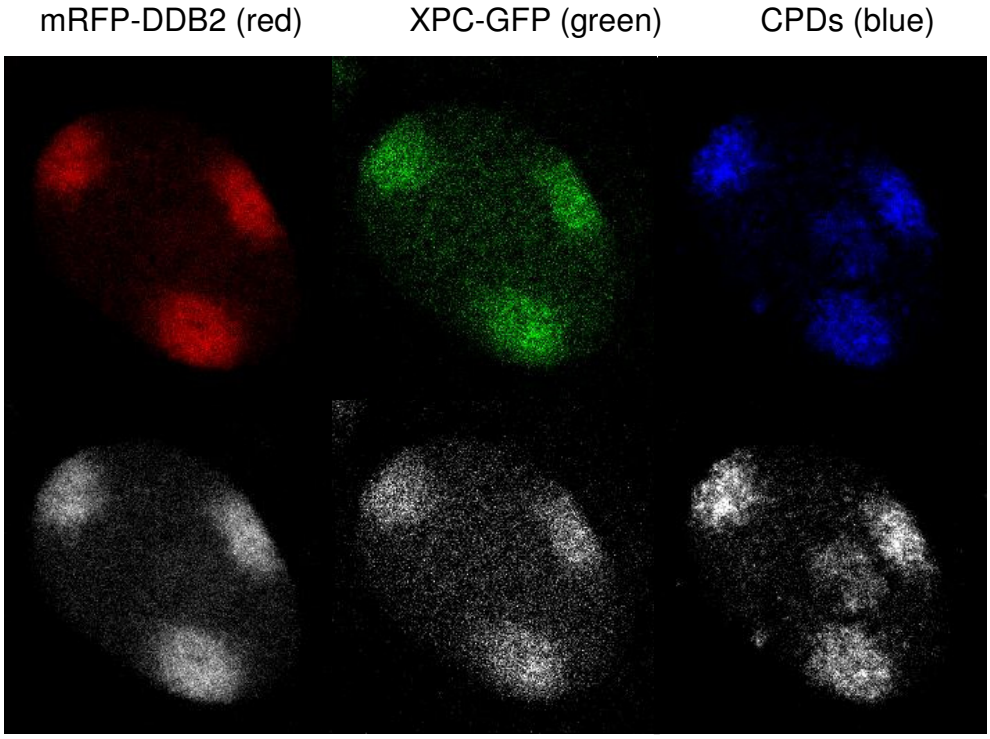

***Figure 18**: Co-localization of mRFP-DDB2 and XPC-GFP in repair foci generated by UV-C irradiation (150 J/m²). Blue, CPDs stained with the dye Alexa fluor 405. Upper panels, original color display of the images; lower panels, black-and-white pictures.*

5.5.2 Co-expression of fluorescent DDB2 and the ubiquitin polypeptide

DDB2 forms a heterodimer with DDB1, which in turn represents a molecular adaptor of the Cul4A-Roc1 ubiquitin ligase complex (Shiyanov *et al*. 1999; Groisman *et al*. 2003; Angers *et al*. 2006; Sugasawa 2009). This DDB-Cul4A-Roc1 ligase promotes the ubiquitylation of protein substrates, *i.e*., it mediates a post-translational modification reaction whereby ubiquitin is covalently linked to proteins (Wilkinson 2000). It is conceivable that, by this ubiquitylation pathway, the DDB1-DDB2 heterodimer may stimulate the proteolytic degradation of proteins cross-linked to DNA (Reardon & Sancar 2006). Thus, to address the possible function of DDB1-DDB2 in the processing of DPXs, we monitored the nuclear ubiquitin turnover in living cells by FRAP analyses. For that purpose, human fibroblasts were co-transfected with mRFP-DDB2 and ubiquitin-GFP (Ubi-GFP).

First, we observed in these nuclear dynamics experiments that the over-expression of DDB2 leads to a slightly decreased mobility of ubiquitin (Figure 19A), consistent with a function of the DDB2 subunit in mediating the covalent ubiquitylation of nuclear proteins. Upon exposure of human fibroblasts to 75 µM FA, the degree of ubiquitin immobilization was enhanced (Figure 19B), lending further support to the conclusion that DDB2 stimulates protein ubiquitylation reactions in response to DPX formation.

(A)

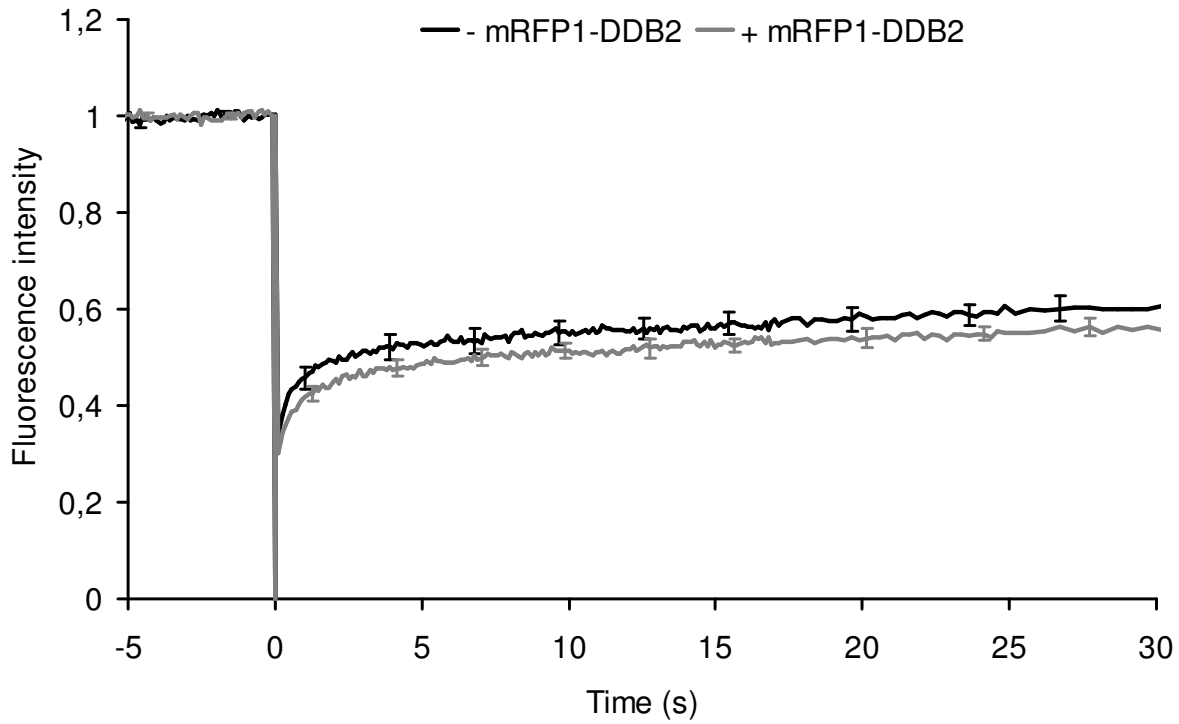
- mRFP1-DDB2
+ mRFP1-DDB2
Fluorescence intensity
1,2
1
0,8
0,6
0,4
0,2
0
-5
0
5
10
15
20
25
30
Time (s)

(B)

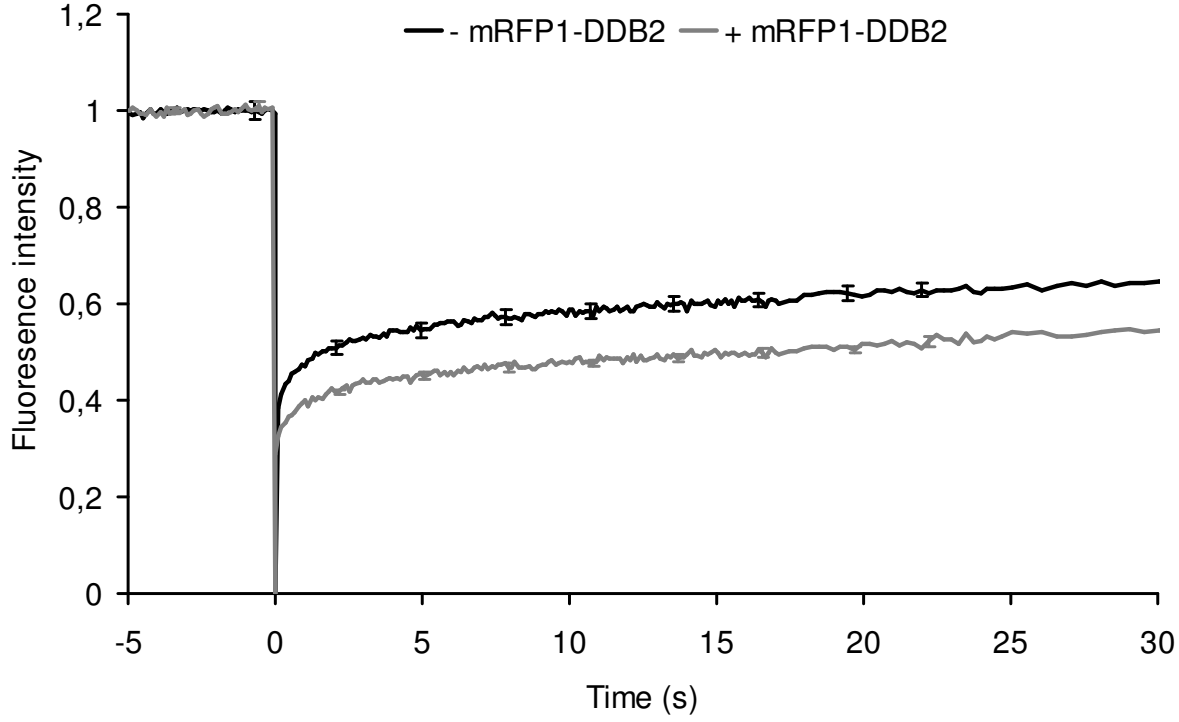
- mRFP1-DDB2
+ mRFP1-DDB2
Fluorescence intensity
1,2
1
0,8
0,6
0,4
0,2
0
-5
0
5
10
15
20
25
30
Time (s)

***Figure 19**: Nuclear dynamics of ubiquitin in human fibroblasts expressing the* **ubiquitin-GFP (Ubi-GFP)** *fusion alone (upper bold line) or in the presence of* **mRFP1-DDB2** *(lower gray line). (A) Untreated cells. (B) Cells exposed to 75 µM FA (n = 10; error bars represent standard errors of the mean).*

5.6 Impairment of NER through DPXs

DDB2 has an exquisite affinity for UV-irradiated DNA and is well known to stimulate the excision of bulky UV-lesions, i.e., CPDs and (6-4) photoproducts, by mediating the recruitment of downstream NER factors (Fitch *et al*. 2003; Moser *et al*. 2005). However, the observed reduced mobility of DDB2 in FA-treated cells (Figure 14) suggests that non-toxic concentrations of FA interfere with the nuclear trafficking of DDB2, such that the repair of UV-induced photoproducts may be indirectly inhibited. Three different experimental methods were employed to test this hypothesis.

5.6.1 Determination of overall UV repair activity in formaldehyde-exposed cells

The possible effect of FA exposure on the removal of UV lesions was first tested using the host-cell reactivation assay. For that purpose, NER-proficient human fibroblasts were transfected with the dual luciferase reporter system, including the UV-damaged reporter vector, as described before (section 4.4). After an 18-h incubation time, the effect of FA treatment was assessed by monitoring the ratio of luciferase activities in cell lysates (Figure 20). No significant inhibition of firefly luciferase expression was observed at a FA concentration of 10 µM. However, the firefly luciferase activity was progressively reduced at FA concentrations of 25–125 µM, thus reflecting an inhibitory effect of this compound on the repair of UV lesions. An approximately 50% inhibition of repair activity was detected at a FA level of 100 µM (Figure 20). Higher concentrations were not tested because, in combination with the transfection procedure, FA levels of 200 µM or above exerted cytotoxic effects (data not shown).

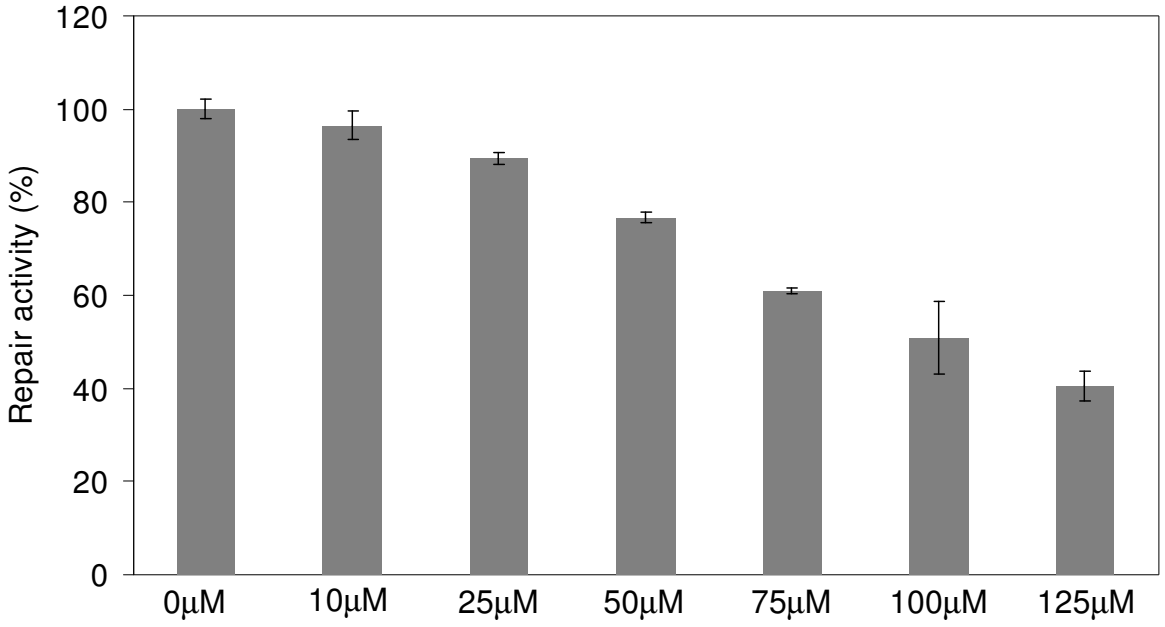

Figure 20*: UV repair activity in fibroblasts determined by host-cell reactivation assay. After transfection in FA-containing medium, cells were treated with different concentrations (0–125 µM) of FA for another 18 hours (n = 12; error bars represent standard deviations).*

5.6.2 Analysis of protein dynamics in UV-irradiated cells

In a next step, we employed FRAP analyses to test how FA affects the nuclear trafficking of DDB2 and XPC in UV-irradiated cells. As already shown in Figure 12, the dynamics of both NER subunits is significantly retarded in UV-irradiated cells, consistent with their role in the detection and repair of UV lesions. Additional exposure to FA did not change the dynamics of the GFP-DDB2 polypeptide (Figure 21A), suggesting that the DDB2 subunit does not discriminate between UV- and FA-induced lesions. In UV-irradiated cells, however, the dynamics of XPC-GFP was changed by the FA treatment, in a way that XPC displays slightly increased protein mobility (Figure 21B). This result obtained in FRAP experiments suggested that the detection of UV lesions by XPC protein may be impeded by FA exposures.

(A)

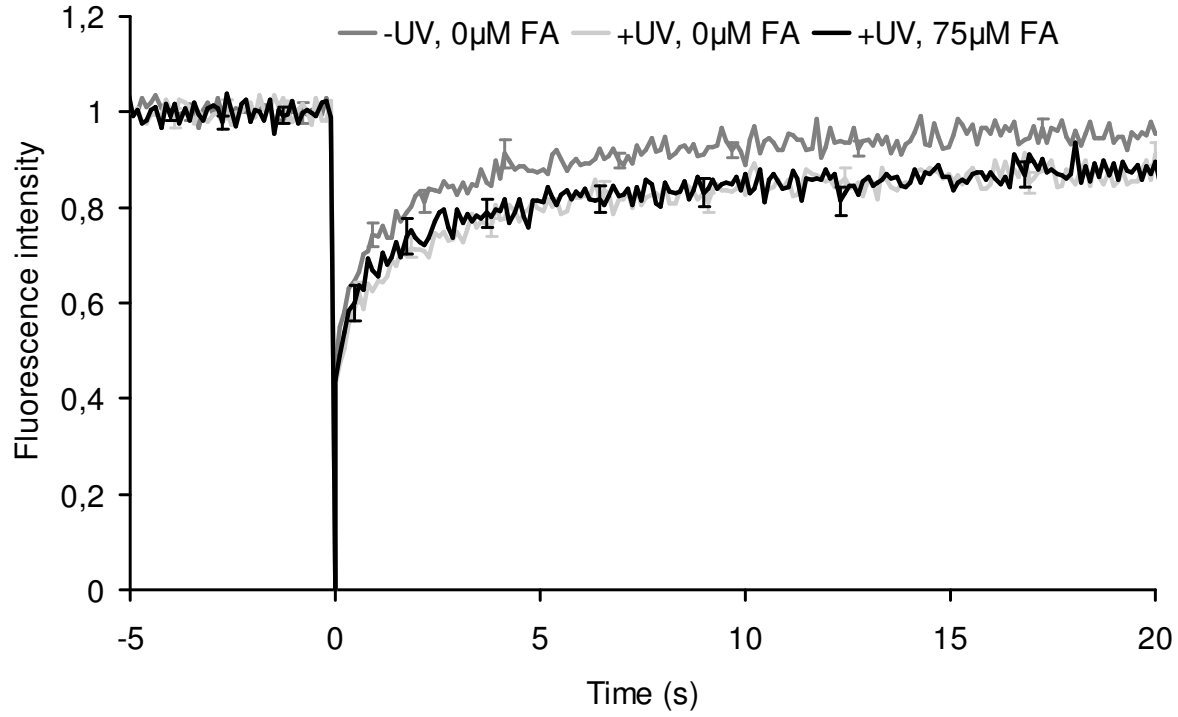
-UV, 0μM FA
+UV, 0μM FA
+UV, 75μM FA
Fluorescence intensity
1,2
1
0,8
0,6
0,4
0,2
0
-5
0
5
10
15
20
Time (s)

(B)

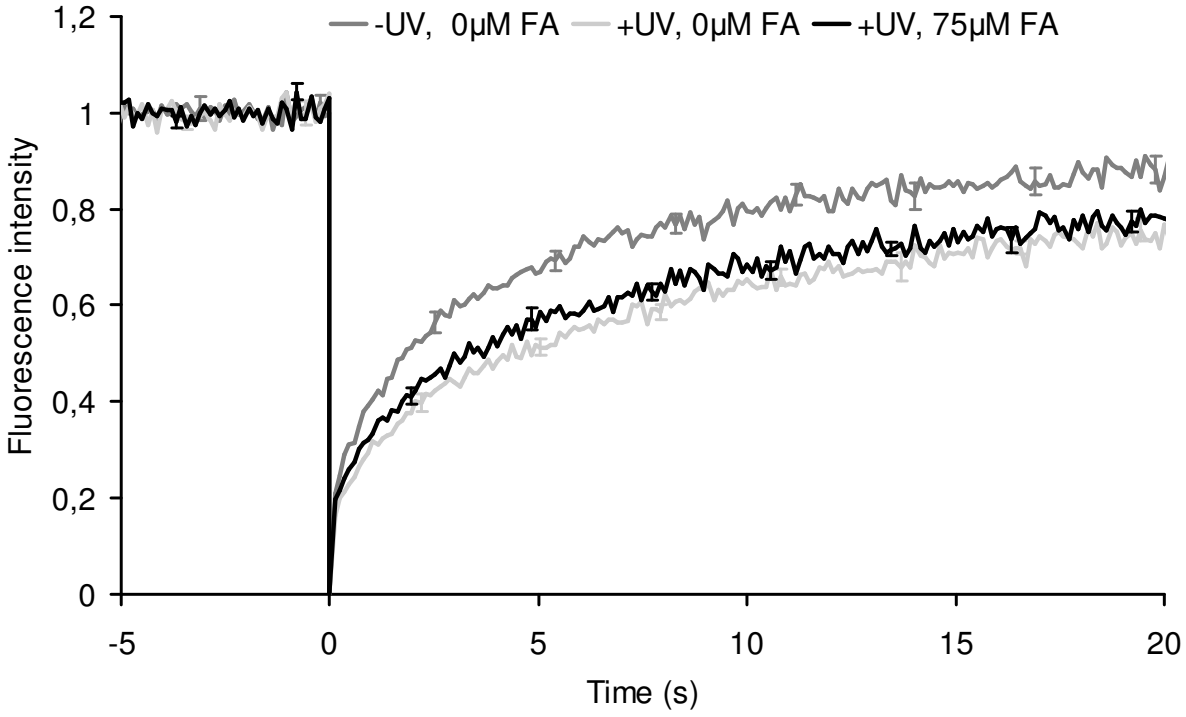
-UV, 0μM FA
+UV, 0μM FA
+UV, 75μM FA
Fluorescence intensity
1,2
1
0,8
0,6
0,4
0,2
0
-5
0
5
10
15
20
Time (s)

***Figure 21**: Effect of a combined UV irradiation and FA treatment on the nuclear dynamics of* **DDB2** *(A) and* **XPC** *protein (B) in human fibroblasts. The UV-C dose was 10 J/m^2 and the FA concentration 75 µM. The dark grey curve represents the protein mobility in the nuclei of untreated cells. The decreased mobility upon UV irradiation is displayed in light grey. The black curve shows the mobility in cells subjected to the combined treatment of UV light and FA.*

5.6.3 Accumulation at local UV-light induced repair foci

To confirm the FA effects observed in FRAP analyses (Figures 14 and Figure 21B), the UV-induced accumulation of DDB2 and XPC was monitored directly in cells locally exposed to UV light (section 4.3). Fibroblasts where transfected with either GFP-DDB2 or XPC-GFP, treated with 100 µM FA for 18 h, and irradiated with UV-C (150 J/m^2) through polycarbonates filters. Subsequently, the cells were fixed and CPDs were stained by cytochemistry. In each case, the accumulation of GFP-tagged proteins in repair foci was determined relative to the fluorescence signal obtained from the immunochemical staining of UV lesions (Figure 22). These quantifications of protein fluorescence relative to the local level of photoproducts showed that FA reduces the ability of DDB2 to accumulate at sites of UV lesions (Figure 22A). Similarly, we found that the FA pretreatment also reduced the efficiency by which XPC protein accumulates in UV-induced repair foci.

(A)

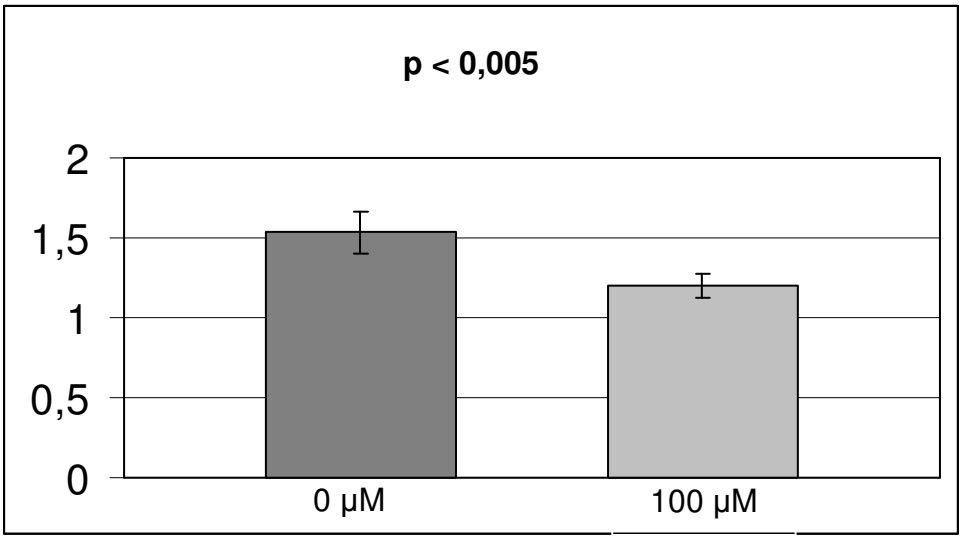

(B)

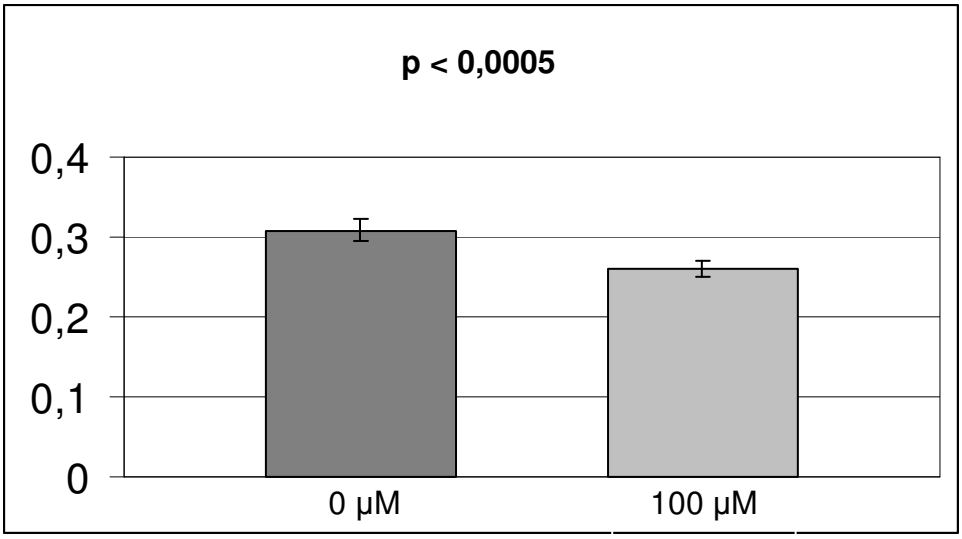

***Figure 22**: Diminished damage-specific accumulation of GFP-DDB2 (A) or XPC-GFP (B) in FA-treated fibroblasts. Human fibroblasts were UV-irradiated through micropore filters and, after an incubation time of 15 min, subjected to immunochemical staining for the visualization of UV lesions (n = 50; error bars represent standard deviations). The GFP signal at the sites of lesions was normalized to the amount of DNA damage. These quantifications showed that FA significantly (p < 0.005) decreases the ability of both DDB2 and XPC to relocate to nuclear areas containing UV photoproducts*.

From these results, we conclude that FA impedes NER activity by interfering with the dynamic trafficking of the recognition factors DDB2 and XPC in the chromatin of living cells. This interference with the normal protein movement leads to the reduced accumulation of the DDB2 and XPC subunits to NER substrates.

6 DISCUSSION

The purpose of the present thesis was to apply different cell biology methods, i.e., host-cell reactivation assay, fluorescence recovery after photobleaching (FRAP) and the induction of fluorescence-based repair foci, to examine the effect of low FA concentrations on DNA repair activity in living human skin fibroblasts. FA is an important industrial raw substance used for the synthesis of chemicals, building materials, home insulation and many consumer goods. Common sources of exposure to this highly reactive compound are, in addition to tobacco smoke, wood products, paints and varnishes, resins used as adhesives and binders, textiles, carpets, leather and disinfectants. As a preservative against bacterial contamination and chemical degradation, cosmetics often contain FA itself or FA-releasing compounds like diazolidinyl urea (Rastogi 2000). The maximal allowed concentration of FA in skin creams regulated by the EU Cosmetic Directive is 0.2% (2 mg/g). Thus, large numbers of people are exposed to FA through the skin, where it easily diffuses into deeper layers (Robbins *et al*. 1984) and often causes contact dermatitis and photosensitivity (Agner *et al*. 1999; Vilaplana & Romaguera 2000). There is no known epidemiological evidence for an increased skin tumor risk due to dermal FA exposure, but an elevated mortality resulting from skin cancers has been reported among embalmers (Walrath & Fraumeni 1983). Another environmental challenge to the human skin is the nearly permanent formation of UV lesions in the DNA resulting from natural sunlight or artificial light sources. Both the UV-B (280 – 315 nm wavelength) and UV-A spectrum (315 – 400 nm wavelength) reach the proliferating cell layer in the skin (Mouret *et al*. 2006) and generate two major classes of mutagenic and carcinogenic DNA photoproducts, i.e., CPDs and 6-4 PPs (described in the Introduction). In human cells, these UV lesions are solely removed via NER system, of which the “global genome repair” (GGR) sub-pathway provides the major protective action against UV-B and UV-A radiation-induced skin cancer (Satoh *et al*. 1993; Reardon *et al*. 1997; Reardon & Sancar 2006; Kuraoka *et al*. 2000). Although many mechanistic details are still highly debated, it is generally thought that the different factors of the GGR machinery are assembled on damaged DNA sites in a sequential and coordinated manner (Volker *et al*. 2001; Politi *et al*. 2005). In particular, the GGR sub-pathway is initiated by the binding of the dimeric DDB protein (consisting of DDB1 and DDB2), followed by the trimeric XPC-RAD23B-CNT2

complex, transcription factor TFIIH (consisting of 10 subunits), XPA, RPA (consisting of 3 subunits) and the two DNA endonucleases XPF-ERCC1 and XPG (Drapkin & Reinberg 1994; O´Donovan *et al*. 1994; Matsunga *et al*. 1995; Bessho *et al*. 1997; Mu *et al*. 1997; de Laat *et al*. 1998; Tang *et al*. 2000; You *et al*. 2003; Camenisch *et al*. 2006). Subsequently, the single-stranded gap resulting from dual DNA incision at lesion sites is processed by further recruitment of a DNA polymerase (δ, ε or κ) together with its accessory factors and a DNA ligase (Shivji *et al*. 1995; Araújo *et al*. 2000). In view of the ability of FA to generate bulky DPXs (Casanova *et al*. 1994; Conaway *et al*. 1996), which may impede macromolecular movements within the nuclear compartment, the present thesis addresses the question of whether exposure to FA interferes with the dynamic trafficking of GGR factors searching for DNA lesions and, hence, retard their coordinated assembly at damaged sites to be repaired. Previous publications reported the inhibitory effect of FA on different DNA repair pathways. For example, DNA damage (O^6-methylguanine) caused by *N*-methyl-*N*-nitrosourea is removed less efficiently from human bronchial cells concomitantly exposed to 100-300 µM FA (Grafstrom 1990). Also, the rejoining of single-stranded DNA breaks after X-ray irradiation was inhibited in the same cells exposed to FA at a concentration level of 100 µM (Grafstrom *et al*. 1983). Exposure of human fibroblasts to 300 µM FA has been estimated by the same authors to generate 2-3 lesions/10^9 daltons, translating to about 1 lesion per 600'000 base pairs (Grafstrom *et al*. 1984). Interestingly, in the study of Grafstrom *et al*. (1983) DNA repair patch synthesis by the NER machinery was also inhibited in the presence of FA. However, substantially higher FA concentrations (600 µM-1 mM) were required to inhibit DNA repair synthesis following the induction of UV lesions or the formation of DNA adducts elicited by the ubiquitous chemical carcinogen benzo[*a*]pyrene diol-epoxide. Thus, these earlier findings indicated that the DNA ligation step (responsible for the direct rejoining of X-ray-induced single-stranded DNA breaks) is more sensitive than the DNA repair synthesis machinery to inhibition upon FA exposure. In a more recent study, Emri *et al*. (2004) used comet (single-cell gel electrophoresis) assays to monitor the transient appearance of single-stranded DNA breaks that were taken as a surrogate indicator of cellular NER activity, which generates DNA incision intermediates, after UV irradiation. They found that human keratinocytes and fibroblasts exposed to low FA concentrations (10-100 µM) prior to UV irradiation showed a delayed kinetics of single-strand break formation after UV-C or UV-B

irradiation. Thus, Emri *et al*. (2004) came to the conclusion that even low FA levels are able to interfere with the assembly of NER complexes at UV lesion sites. In the present thesis, we used a highly specific host-cell reactivation assay to confirm the inhibitory action of FA on the repair of UV lesions. This assay determines the proficiency of human cells in recruiting the NER system to remove UV lesions from a luciferase reporter gene sequence, thus reactivating expression of an easily detectable luciferase enzyme. This approach demonstrated that the overall NER activity is significantly reduced in the presence of 25 µM FA, whereas an approximately 50% inhibition of repair activity was detected at a FA concentration of 75 µM (Fig. 20). This host-cell reactivation assay yielded a no-effect-level of 10 µM. Two different lines of evidence support the conclusion that this low-dose FA effect on the excision of UV lesions arises from an impaired nuclear trafficking of GGR factors in UV-irradiated cells. Using the FRAP technique, we observed that the mobility of DDB2 protein (tested as a green-fluorescent fusion construct) is significantly reduced in cells exposed to 75 µM FA compared to the untreated controls (Fig. 14). This difference in fluorescence recovery indicates that the overall diffusion rate of DDB2 protein is diminished upon FA treatment, implying that in response to the FA-induced formation of DPXs this initial recognition factor may be retarded in its molecular movements necessary to reach UV-damaged DNA sites within the nuclear compartment. This view is consistent with the finding that the accumulation of DDB2 protein (tested again as a green-fluorescent fusion construct) in foci of local UV damage was significantly reduced upon FA treatment (Fig. 22). A lower accumulation in locally UV-irradiated nuclear areas was also observed for XPC protein (Fig. 22), which is an interaction partner of DDB2 and another key sensor of DNA damage in the NER pathway (see “Introduction”). Taken together, these results suggest that FA-induced DPXs interfere with the normal dynamic trafficking of two different guardians of DNA integrity (DDB and XPC proteins) that act as the initial damage detectors in the GGR process. In the cellular context, DDB2 is always present in association with DDB1, which is a molecular adapter for the Cul4A-Roc1 ubiquitin ligase complex (Shiyanov *et al*. 1999) and, hence, mediates the ubiquitylation of target proteins (Nag *et al*. 2001; Sugasawa *et al*. 2005). Therefore, we tested whether the DDB1-DDB2 dimer may stimulate the ubiquitylation of proteins following FA treatments. Ubiquitylation is a post-translational protein modification that may serve to initiate the degradation of cross-linked proteins by the proteasomal complex (Hochstrasser

1996). To address the possible function of DDB1-DDB2 in the ubiquitylation process following the formation of DPXs, we used the FRAP analysis to monitor the nuclear ubiquitin turnover in living cells. These experiments were made possible by a genetic construct, in which the ubiquitin moiety is fused to green fluorescent protein. First, we observed that the over-expression of DDB2 leads to a reduced nuclear mobility of ubiquitin (Figure 19A), consistent with a function of the DDB2 subunit in mediating the ubiquitylation of proteins, thus decreasing the pool of free nuclear ubiquitin. Upon exposure of human fibroblasts to 75 µM FA, the immobilization of ubiquitin by expression of DDB2 was further enhanced (Figure 19B), indicating that DDB2 stimulates protein ubiquitylation reactions in response to DPX formation.

The results of the present thesis provide an alternative mechanism that may explain how low-dose FA treatments delay the GGR response following UV irradiation. According to our findings, the observed inhibitory effect of FA on the repair of UV lesions is caused at least in part by the impaired trafficking of GGR factors, leading to their delayed recruitment to lesion sites, rather than by a catalytic slow-down of enzymes involved in the synthesis of repair patches or the final DNA ligation step. In a wider perspective, such an impairment of DNA repair, affecting the removal of mutagenic lesions arising from both endogenous and exogenous agents, may help to explain the wide spectrum of genotoxic effects exerted by FA. In fact, this compound has been shown to induce DNA strand breaks, sister-chromatid exchanges, chromosomal aberrations leading to micronuclei formation, as well as point mutations (Natarajan *et al*. 1983; Craft *et al*. 1987; Crosby *et al*. 1988; Recio *et al*. 1992; Merk & Speit 1998). DNA strand breaks, sister-chromatid exchanges and micronuclei are generated in the same concentration range that also causes a reduction in cloning efficiency, indicating that these clastogenic effects of FA are inherently related to the ability of DPXs to disrupt the DNA replication machinery or subsequent mitotic processes (Merk & Speit 1998; Heck & Casanova 1999). On the other hand, it is uncertain how FA induces point mutations (mainly base transversions) as they have been found in the *p53* tumor suppressor gene of FA-induced nasal tumors in rats (Recio *et al*. 1992). The observed inhibition of DNA repair following FA exposure may result in the replication of incompletely repaired DNA templates that, in turn, may give rise to such tumorigenic base transversions or other point mutations. In any case, a synergistic effect may be expected when the skin is concomitantly exposed to FA and UV light from natural or artificial sources. A reduced DNA repair activity due to the

interference of FA-induced DPXs with the nuclear dynamics of individual GGR factors is likely to enhance the photo-carcinogenic risk to humans.

7 REFERENCES

- Andressoo JO, Hoeijmakers JH (2005) „Transcription-coupled repair and premature ageing.“ Mutat Res 577:179-94.
- Agner T, Flyvholm MA, Menne T (1999) “Formaldehyde allergy: a follow-up study.” Am J Contact Dermat 10:12-17.
- Angers S, Li T, Yi X, MacCoss MJ, Moon RT, Zheng N (2006) “Molecular architecture and assembly of the DDB1-CUL4A ubiquitin ligase machinery.” Nature. 443:590-3.
- Araújo SJ, Tirode F, Coin F, Pospiech H, Syväoja JE, Stucki M, Hübscher U, Egly JM, Wood RD (2000) “Nucleotide excision repair of DNA with recombinant human proteins: definition of the minimal set of factors, active forms of TFIIH, and modulation by CAK.” Genes Dev. 14:349-59.
- Baird GS, Zacharias DA, Tsien RY (2000) “Biochemistry, mutagenesis, and oligomerization of DsRed, a red fluorescent protein from coral.” Proc Natl Acad Sci 97:11984-9.
- Barker S, Weinfeld M, Murray D (2005) “DNA-protein crosslinks: their induction, repair, and biological consequences.” Mutat Res. 589:111-35.
- Baute J, Depicker A (2008) “Base excision repair and its role in maintaining genome stability.” Crit Rev Biochem Mol Biol. 43:239-76.
- Bergstralh DT, Sekelsky J. (2008) “Interstrand crosslink repair: can XPF-ERCC1 be let off the hook?” Trends Genet. 24:70-6.
- Bessho T, Sancar A, Thompson LH, Thelen MP (1997) „Reconstitution of human excision nuclease with recombinant XPF-ERCC1 complex.“ J Biol Chem. 272:3833-7.
- Bevis BJ, Glick BS. (2002) “Rapidly maturing variants of the Discosoma red fluorescent protein (DsRed).” Nat Biotechnol. 20:83-7. Erratum in: Nat Biotechnol. 20:1159.
- Bienstock RJ, Skorvaga M, Mandavilli BS, Van Houten B (2003) „Structural and functional characterization of the human DNA repair helicase XPD by comparative molecular modeling and site-directed mutagenesis of the bacterial repair protein UvrB.“ J Biol Chem. 278:5309-16.
- Buterin T, Meyer C, Giese B, Naegeli H (2005) „DNA quality control by

conformational readout on the undamaged strand of the double helix.“ Chem Biol. 12:913-22.

- Camenisch U, Dip R, Schumacher SB, Schuler B, Naegeli H (2006) „ Recognition of helical kinks by xeroderma pigmentosum group A protein triggers DNA excision repair.“ Nat Struct Mol Biol. 13:278-84.
- Camenisch U, Dip R, Vitanescu M, Naegeli H (2007) „ Xeroderma pigmentosum complementation group A protein is driven to nucleotide excision repair sites by the electrostatic potential of distorted DNA.“ DNA Repair (Amst) 6:1819-28.
- Camenisch U, Naegeli H (2009) “Role of DNA repair in the protection against genotoxic stress." EXS. 99:111-50.
- Campbell RE, Tour O, Palmer AE, Steinbach PA, Baird GS, Zacharias DA, Tsien RY (2002) “A monomeric red fluorescent protein.” Proc Natl Acad Sci 99(12):7877-82
- Cardarelli F, Bizzarri R, Serresi M, Albertazzi L, Beltram F (2009) “Probing nuclear localization signal-importin alpha binding equilibria in living cells.” J Biol Chem. 284:36638-46.
- Carreau M, Eveno E, Quilliet X, Chevalier-Lagente O, Benoit A, Tanganelli B, Stefanini M, Vermeulen W, Hoeijmakers JH, Sarasin A, et al.(1995) “Development of a new easy complementation assay for DNA repair deficient human syndromes using cloned repair genes.” Carcinogenesis 16:1003-9.
- Carrero G, McDonald D, Crawford E, de Vries G, Hendzel MJ (2003) Using FRAP and mathematical modelling to determine the in vivo kinetics of nuclear proteins. Methods 29:14-28.
- Casanova M, Heck HD, Everitt JI, Harrington WW Jr, Popp JA (1988) “Formaldehyde concentrations in the blood of rhesus monkeys after inhalation exposure.” Food Chem Toxicol. 26:715-6.
- Casanova M, Morgan KT, Steinhagen WT, Everitt JI, Popp JA and Heck Hd´ A (1991) „Covalent binding of inhaled formaldehyde to DNA in the respiratory tract of rhesus monkeys: pharmacokinetics, rat-to-monkey interspecies scaling and extrapolation to man” Fundam Appl Toxicol. 17: 409-428.
- Casanova M, Morgan KT, Gross EA, Moss OR and Heck Hd´A (1994) “DNA-protein cross link and cell replication at specific sites in the nose of F344 rats

exposed subchronically to formaldehyde" Fundam Appl Toxicol. 23: 525-536.

- Casteel SW, Vernon RJ, Bailey EM Jr. (1987) „Formaldehyde: toxicology and hazards.“ Vet Hum Toxicol. 29: 31-33.
- Chalfie M, Tu Y, Euskirchen G, Ward WW, Prasher DC (1994) "Green fluorescent protein as a marker for gene expression." Science 263(5148):802-5.
- Chen Z, Xu XS, Yang J, Wang G (2003) „ Defining the function of XPC protein in psoralen and cisplatin-mediated DNA repair and mutagenesis.“ Carcinogenesis. 24:1111-21.
- CIIT (Chemical Industry Institute of Toxicology) (1999) "Formaldehyde: Hazard Characterization and Dose-Response Assessment for Carcinogenicity by Route of Inhalation.“ Centers for Health Research. Research Triangle Park, MD.
- Cohen SM, Lippard SJ (2001) „ Cisplatin: from DNA damage to cancer chemotherapy.“ Prog Nucleic Acid Res Mol Biol. 67:93-130.
- Conaway CC, Whysner J, Verna LK, Williams GM (1996) "Formaldehyde mechanistic data and risk assessment: endogenous protection from DNA adduct formation." Pharmacol Ther. 71(1-2):29-55.
- Cormack BP, Valdivia RH, Falkow S (1996) "FACS-optimized mutants of the green fluorescent protein (GFP)." Gene. 173:33-8.
- CPSC (Consumer product safety commission) (U.S.) (1997) "An Update on formaldehyde" (Document 725)
- Craft TR, Bermudez E, Skopek TR (1987) "Formaldehyde mutagenesis and formation of DNA-protein crosslinks in lymphoblasts in vitro." Mutat Res 176: 147-155.
- Crosby RM, Richardson KK, Craft TR, Benforado KB, Liber HL, Skopek TR (1988) "Molecular analysis of formaldehyde-induced mutations in human lymphoblasts and E. coli." Environ Mol Mutagen 12:155-166
- Dallas CE, Theiss JC, Harrist RB, Fairchild EJ (1985) "Effect of subchronic foraldehyde inhalation on minute volume and nasal deposition in Sprague-Dawley rats" J Toxicol Environ Health. 16: 553-64.
- Dantuma NP, Groothuis TA, Salomons FA, Neefjes J (2006) A dynamic ubiquitin equilibrium couples proteasomal activity to chromatin remodeling. J

Cell Biol. 173:19-26.

- Day RN, Schaufele F (2006) “Imaging molecular interactions in living cells.” Molecular Endocrinology 19 (7), 1675.
- Day RN, Schaufele F (2008) “Fluorescent protein tools for studying protein dynamics in living cells: a review.” J Biomed Opt. 13:031202.
- de Boer J, Hoeijmakers JH. (2000) “Nucleotide excision repair and human syndromes.” Carcinogenesis. 21:453-60.
- de Laat WL, Appeldoorn E, Sugasawa K, Weterings E, Jaspers NG, Hoeijmakers JH (1998) „DNA-binding polarity of human replication protein A positions nucleases in nucleotide excision repair.“ Genes Dev. 12:2598-609.
- D'Errico M, Parlanti E, Teson M, de Jesus BM, Degan P, Calcagnile A, Jaruga P, Bjørås M, Crescenzi M, Pedrini AM, Egly JM, Zambruno G, Stefanini M, Dizdaroglu M, Dogliotti E (2006) „New functions of XPC in the protection of human skin cells from oxidative damage.“ EMBO J. 25:4305-15.
- Dip R, Camenisch U, Naegeli H (2004) “Mechanisms of DNA damage recognition and strand discrimination in human nucleotide excision repair.” DNA Repair (Amst). 3:1409-23.
- Drapkin R, Reinberg D (1994) „The multifunctional TFIIH complex and transcriptional control.“ Trends Biochem Sci. 19:504-8.
- Edidin M, Zagyansky Y and Lardner TJ (1976) “Measurement of membrane protein lateral
- Emri G, Schaefer D, Held B, Herbst C, Zieger W, Horkay I, Bayerl C (2004) “Low concentrations of formaldehyde induce DNA damage and delay DNA repair after UV irradiation in human skin cells.” Exp Dermatol 13:305-315.
- Enzlin JH, Schärer OD (2002) “The active site of the DNA repair endonuclease XPF-ERCC1 forms a highly conserved nuclease motif." EMBO J. 21:2045-53.
- Fitch ME, Nakajima S, Yasui A, Ford JM (2003) „In vivo recruitment of XPC to UV-induced cyclobutane pyrimidine dimers by the DDB2 gene product.“ J Biol Chem. 278:46906-10.
- Fousteri M, Vermeulen W, van Zeeland AA, Mullenders LH (2006) “Cockayne syndrome A and B proteins differentially regulate recruitment of chromatin remodeling and repair factors to stalled RNA polymerase II in vivo.” Mol Cell. 23:471-82.

- Friedberg EC, Walker GC, Siede W, Wood RD, Schultz RA, Ellenberger T (2006) „DNA Repair and Mutagenesis“ ASM Press. Washington DC
- Fujiwara Y, Masutani C, Mizukoshi T, Kondo J, Hanaoka F, Iwai S (1999) “Characterization of DNA recognition by the human UV-damaged DNA-binding protein.” J Biol Chem. 274:20027-33.
- Furuta T, Ueda T, Aune G, Sarasin A, Kraemer KH, Pommier Y (2002) „ Transcription-coupled nucleotide excision repair as a determinant of cisplatin sensitivity of human cells.“ Cancer Res. 62:4899-902.
- Fuselli S, Zanetti C (2006) “Formaldehyde in air of indoor and outdoor environments of urban area, relationships man's exposure” Ann Ist Super Sanita. 42:365-8. Italian.
- Gierasch LM, Gershenson A (2009) “Post-reductionist protein science, or putting Humpty Dumpty back together again.” Nat Chem Biol. 5:774-7.
- Grafstrom RC, Fornace AJ, Autrup H, Lechner JF, Harris CC (1983) “Formaldehyde damage to DNA and inhibition of DNA repair in human bronchial cells.” Science 220:216-218.
- Grafstrom RC, Fornace AJ, Harris CC (1984) “Repair of DNA damage caused by formaldehyde in human cells.” Cancer Res 44:4323-4327.
- Grafstrom RC (1990) “In vitro studies of aldehyde effects related to human respiratory carcinogenesis.” Mutat Res 238:175-184.
- Greene Mh (1992) “Is cisplatin a human carcinogen?” J Nat Cancer Inst 306-12
- Groisman R, Polanowska J, Kuraoka I, Sawada J, Saijo M, Drapkin R, Kisselev AF, Tanaka K, Nakatani Y (2003) “The ubiquitin ligase activity in the DDB2 and CSA complexes is differentially regulated by the COP9 signalosome in response to DNA damage.” Cell. 113:357-67.
- Gross LA, Baird GS, Hoffman RC, Baldridge KK, Tsien RY (2000) “The structure of the chromophore within DsRed, a red fluorescent protein from coral.” Proc Natl Acad Sci U S A. 97:11990-5.
- Hanawalt PC (2002) “Subpathways of nucleotide excision repair and their regulation." Oncogene. 21:8949-56.
- Hauptmann M, Lubin JH, Stewart PA, Hayes RB, Blair A (2003) “Mortality from lymphohematopoietic malignancies among workers in formaldehyde

industries.” J Natl Cancer Inst. 95:1615-23.

- Hauptmann M, Lubin JH, Stewart PA, Hayes RB, Blair A (2004) “Mortality from solid cancers among workers in formaldehyde industries.” Am J Epidemiol. 159:1117-30.
- Heck, HD, Chin, TY and Schmitz, MC (1983) „Distribution of (14C) formaldehyde in rats after inhalation exposure.“ Formaldehyde toxicity, Hemisphere Publishing, Washington, DC, pp. 26–37.
- Heck HD, Casanova-Schmitz M, Dodd PB, Schachter EN, Witek TJ, Tosum T (1985) “Formaldehyde concentrations in the blood of humans and Ficher-344 rats exposed to formaldehyde under controlled conditions.” Am Ind Hyg Assoc J. 46:1-3.
- Heck HD, Keller DA (1988) “Toxicology of formaldehyde.” ISI Atlas Sci. Pharmacol. 2:5-9.
- Heck H, Casanova M (1999) “Pharmacodynamics of formaldehyde: applications of a model for the arrest of DNA replication by DNA-protein crosslinks.” Toxicol Appl Pharmacol 160:86-100.
- Heck H, Casanova M. (2004) “The implausibility of leukemia induction by formaldehyde: a critical review of the biological evidence on distant-site toxicity.” Regul Toxicol Pharmacol. 40:92-106.
- Heim R, Tsien RY (1996) “Engineering green fluorescent protein for improved brightness, longer wavelengths and fluorescence resonance energy transfer.” Curr Biol. 6(2):178-82
- Hirschfeld S, Levine AS, Ozato K, Protić M (1990) „ A constitutive damage-specific DNA-binding protein is synthesized at higher levels in UV-irradiated primate cells.“ Mol Cell Biol. 10:2041-8.
- Hochstrasser M. (1996) “Ubiquitin-dependent protein degradation.” Annu Rev Genet. 30:405-39.
- Hoogstraten D, Bergink S, Ng JM, Verbiest VH, Luijsterburg MS, Geverts B, Raams A, Dinant C, Hoeijmakers JH, Vermeulen W, Houtsmuller AB (2008) “Versatile DNA damage detection by the global genome nucleotide excision repair protein XPC.” J Cell Sci. 121:2850-9
- Houtsmuller AB, Rademakers S, Nigg AL, Hoogstraten D, Hoeijmakers JH and Vermeulen W (1999). “Action of DNA repair endonuclease ERCC1/XPF in

living cells.” Science 284, 958-961.

- Hubal EA, Schlosser PM, Conolly RB, Kimbell JS (1997) “Comparison of inhaled formaldehyde dosimetry predictions with DNA-protein cross-link measurements in the rat nasal passages.” Toxicol Appl Pharmacol. 143:47-55.
- Hwang BJ, Ford JM, Hanawalt PC, Chu G (1999) “Expression of the p48 xeroderma pigmentosum gene is p53-dependent and is involved in global genomic repair.“ Proc Natl Acad Sci U S A. 96:424-8.
- Ide H, Nakano T, Salem AM, Terato H, Pack SP, Makino K (2008) “Repair of DNA-protein crosslink damage: coordinated actions of nucleotide excision repair and homologous recombination." Nucleic Acids Symp Ser (Oxf). 52:57-8.
- International agency for research on cancer (IARC) (2004) „ Monographs on formaldehyde, 2-butoxyethanol, and 1-tert-butoxy-2-propanol.“
- Kalla S, Stern M, Basu J, Varoqueaux F, Reim K, Rosenmund C, Ziv NE, Brose N (2006) “Molecular dynamics of a presynaptic active zone protein studied in Munc13-1-enhanced yellow fluorescent protein knock-in mutant mice.” J Neurosci. 26:13054-66.
- Keeney S, Eker AP, Brody T, Vermeulen W, Bootsma D, Hoeijmakers JH, Linn S (1994) „ Correction of the DNA repair defect in xeroderma pigmentosum group E by injection of a DNA damage-binding protein.“ Proc Natl Acad Sci U S A. 91:4053-6.
- Kielbassa C, Roza L, Epe B (1997) „ Wavelength dependence of oxidative DNA damage induced by UV and visible light.“ Carcinogenesis. 18:811-6.
- Kim JK, Patel D, Choi BS (1995) „ Contrasting structural impacts induced by cis-syn cyclobutane dimer and (6-4) adduct in DNA duplex decamers: implication in mutagenesis and repair activity.“ Photochem Photobiol. 62:44-50.
- Kraemer KH, Lee MM, Scotto J (1984) „DNA repair protects against cutaneous and internal neoplasia: evidence from xeroderma pigmentosum.“ Carcinogenesis. 5:511-4.
- Kuraoka I, Bender C, Romieu A, Cadet J, Wood RD, Lindahl T (2000) “Removal of oxygen free-radical-induced 5',8-purine cyclodeoxynucleosides from DNA by the nucleotide excision-repair pathway in human cells.“ Proc Natl

Acad Sci U S A. 97:3832-7.

- Kusumoto R, Masutani C, Sugasawa K, Iwai S, Araki M, Uchida A, Mizukoshi T, Hanaoka F (2001) „ Diversity of the damage recognition step in the global genomic nucleotide excision repair in vitro.“ Mutat Res. 485:219-27.
- Li X, Zhang G, Ngo N, Zhao X, Kain SR, Huang CC (1997) “Deletions of the Aequorea victoria green fluorescent protein define the minimal domain required for fluorescence.” J Biol Chem. ;272:28545-9.
- Li X, Heyer WD (2008) “Homologous recombination in DNA repair and DNA damage tolerance.” Cell Res. 18:99-113.
- Lopes M, Foiani M, Sogo JM (2006) “Multiple mechanisms control chromosome integrity after replication fork uncoupling and restart at irreparable UV lesions.” Mol Cell. 21:15-27.
- Luijsterburg MS, Goedhart J, Moser J, Kool H, Geverts B, Houtsmuller AB, Mullenders LH, Vermeulen W, van Driel R (2007) “Dynamic in vivo interaction of DDB2 E3 ubiquitin ligase with UV-damaged DNA is independent of damage-recognition protein XPC.” J Cell Sci. 120:2706-16.
- Ma TH, Harris MM (1988) “Review of the genotoxicity of formaldehyde” Mutat Res. 196:37-59.
- Maddukuri L, Dudzińska D, Tudek B (2007) “Bacterial DNA repair genes and their eukaryotic homologues: 4. The role of nucleotide excision DNA repair (NER) system in mammalian cells.” Acta Biochim Pol. 54:469-82.
- Maillard O, Camenisch U, Clement FC, Blagoev KB, Naegeli H (2007) „DNA repair triggered by sensors of helical dynamics.“ Trends Biochem Sci. 32:494-9.
- Marcsek ZL, Kocsis Z, Szende B, Tompa A. (2007) “Effect of formaldehyde and resveratrol on the viability of Vero, HepG2 and MCF-7 cells.“ Cell Biol Int. 31:1214-9.
- Matsunaga T, Mu D, Park CH, Reardon JT, Sancar A (1995) „Human DNA repair excision nuclease. Analysis of the roles of the subunits involved in dual incisions by using anti-XPG and anti-ERCC1 antibodies.“ J Biol Chem. 270:20862-9.
- Matz MV, Fradkov AF, Labas YA, Savitsky AP, Zaraisky AG, Markelov ML, Lukyanov SA (1999) “Fluorescent proteins from nonbioluminescent Anthozoa

species.” Nat Biotechnol. 17(10):969-73.

- McAteer K, Jing Y, Kao J, Taylor JS, Kennedy MA (1998) “Solution-state structure of a DNA dodecamer duplex containing a Cis-syn thymine cyclobutane dimer, the major UV photoproduct of DNA.” J Mol Biol. 282:1013-32.
- Meador JA, Walter RB, Mitchell DL (2000) „Induction, distribution and repair of UV photodamage in the platyfish, Xiphophorus signum.“ Photochem Photobiol. 72:260-6.
- Merk O and Speit G (1998) “Significance of formaldehyde induced DNA-protein cross links for mutagenesis” Environ Mol Mutagen. 32: 260-268.
- Minko IG, Zou Y, Lloyd RS (2002) “Incision of DNA-protein crosslinks by UvrABC nuclease suggests a potential repair pathway involving nucleotide excision repair.” Proc Natl Acad Sci U S A. 99:1905-9.
- Mitchell JR, Hoeijmakers JH, Niedernhofer LJ (2003) “Divide and conquer: nucleotide excision repair battles cancer and ageing.” Curr Opin Cell Biol. 15:232-40.
- Mladenova V, Russev G (2008) “DNA interstrand crosslinks repair in mammalian cells.” Z Naturforsch C. 63:289-96.
- Moggs JG, Yarema KJ, Essigmann JM, Wood RD (1996) „ Analysis of incision sites produced by human cell extracts and purified proteins during nucleotide excision repair of a 1,3-intrastrand d(GpTpG)-cisplatin adduct.“ J Biol Chem. 271:7177-86.
- Moggs JG, Szymkowski DE, Yamada M, Karran P, Wood RD (1997) “Differential human nucleotide excision repair of paired and mispaired cisplatin-DNA adducts.” Nucleic Acids Res. ;25:480-91.
- Morise H, Shimomura O, Johnson FH, Winant J (1974) “Intermolecular energy transfer in the bioluminescent system of Aequorea.” Biochemistry. 13:2656-62.
- Moser J, Volker M, Kool H, Alekseev S, Vrieling H, Yasui A, van Zeeland AA, Mullenders LH (2005) “The UV-damaged DNA binding protein mediates efficient targeting of the nucleotide excision repair complex to UV-induced photo lesions.“ DNA Repair (Amst). 4:571-82.
- Mouret S, Baudouin C, Charveron M, Favier A, Cadet J, Douki T (2006) “Cyclobutane pyrimidine dimers are predominant DNA lesions in whole human

skin exposed to UVA radiation.“ Proc Natl Acad Sci U S A. 103:13765-70.

- Mu D, Wakasugi M, Hsu DS, Sancar A (1997) „Characterization of reaction intermediates of human excision repair nuclease.“ J Biol Chem. 272:28971-9.
- Nag A, Bondar T, Shiv S, Raychaudhuri P (2001) „ Nag The xeroderma pigmentosum group E gene product DDB2 is a specific target of cullin 4A in mammalian cells.“ Mol Cell Biol. 21:6738-47.
- Natarajan AT, Darroudi F, Bussman CJ, van Kesteren-van Leuwen AC (1983) “Evaluation of the mutagenicity of formaldehyde in mammalian cytogenetic assays in vivo an vitro.” Mutat Res 122:355-360.
- Naya M, Nakanishi J (2005) “Risk assessment of formaldehyde for the general population in Japan.” Regul Toxicol Pharmacol. 43:232-48.
- Ng JM, Vermeulen W, van der Horst GT, Bergink S, Sugasawa K, Vrieling H, Hoeijmakers JH (2003) „A novel regulation mechanism of DNA repair by damage-induced and RAD23-dependent stabilization of xeroderma pigmentosum group C protein.“ Genes Dev. 17:1630-45.
- Nishi R, Okuda Y, Watanabe E, Mori T, Iwai S, Masutani C, Sugasawa K, Hanaoka F (2005) “Centrin 2 stimulates nucleotide excision repair by interacting with xeroderma pigmentosum group C protein.“ Mol Cell Biol. 25:5664-74.
- Nouspikel T (2009) “DNA repair in mammalian cells : Nucleotide excision repair: variations on versatility." Cell Mol Life Sci. 66:994-1009.
- O'Donovan A, Davies AA, Moggs JG, West SC, Wood RD (1994) „XPG endonuclease makes the 3' incision in human DNA nucleotide excision repair.“ Nature. 371:432-5.
- Ormö M, Cubitt AB, Kallio K, Gross LA, Tsien RY, Remington SJ (1996) “Crystal structure of the Aequorea victoria green fluorescent protein.” Science. 273:1392-5.
- Oro J and Rappoport DA (1959) „Formate metabolism by animal tissues. II. The mechanism of formate oxidation“ J. Biol. Chem. 234: 1661-1665
- Perdiz D, Grof P, Mezzina M, Nikaido O, Moustacchi E, Sage E (2000) „Distribution and repair of bipyrimidine photoproducts in solar UV-irradiated mammalian cells. Possible role of Dewar photoproducts in solar mutagenesis.“ J Biol Chem. 275:26732-42.

- Pfeifer GP (1997) “Formation and processing of UV photoproducts: effects of DNA sequence and chromatin environment.“ Photochem Photobiol. 65:270-83.
- Politi A, Moné MJ, Houtsmuller AB, Hoogstraten D, Vermeulen W, Heinrich R, van Driel R (2005) “Mathematical modeling of nucleotide excision repair reveals efficiency of sequential assembly strategies.” Mol Cell. 19:679-90.
- Quievryn G, Zhitkovich A (2000) “Loss of DNA-protein crosslinks from formaldehyde-exposed cells occurs through spontaneous hydrolysis and an active repair process linked to proteosome function.” Carcinogenesis. 21:1573-80.
- Rademakers S, Volker M, Hoogstraten D, Nigg AL, Moné MJ, Van Zeeland AA, Hoeijmakers JH, Houtsmuller AB, Vermeulen W (2003) “Xeroderma pigmentosum group A protein loads as a separate factor onto DNA lesions.” Mol Cell Biol. 23:5755-67.
- Rabik CA, Dolan ME (2007) “Molecular mechanisms of resistance and toxicity associated with platinating agents.” Cancer Treat Rev. 33:9-23..
- Rapić-Otrin V, Navazza V, Nardo T, Botta E, McLenigan M, Bisi DC, Levine AS, Stefanini M (2003) „ True XP group E patients have a defective UV-damaged DNA binding protein complex and mutations in DDB2 which reveal the functional domains of its p48 product.“ Hum Mol Genet. 12:1507-22.
- Rastogi SC (2000) “Analytical control of preservative labeling on skin creams.” Contact Dermatitis 43:339-343.
- Reardon JT, Bessho T, Kung HC, Bolton PH, Sancar A (1997) “In vitro repair of oxidative DNA damage by human nucleotide excision repair system: possible explanation for neurodegeneration in xeroderma pigmentosum patients.“ Proc Natl Acad Sci U S A. 94:9463-8.
- Reardon JT, Sancar A (2006) “Repair of DNA-polypeptide crosslinks by human excision nuclease.“ Proc Natl Acad Sci U S A.103:4056-61.
- Recio L, Sisk S, Pluta L, Bermudez E, Gross EA, Chen Z, Morgan K, Walker C (1992) “p53 Mutations in formaldehyde-induced squameous cell carcinomas in rats.” Cancer Res 52:6113-6116.
- Ridpath JR, Nakamura A, Tano K, Luke AM, Sonoda E, Arakawa H, Buerstedde JM, Gillespie DA, Sale JE, Yamazoe M, Bishop DK, Takata M,

Takeda S, Watanabe M, Swenberg JA, Nakamura J (2007) “Cells deficient in the FANC/BRCA pathway are hypersensitive to plasma levels of formaldehyde.” Cancer Res. 67:11117-22.

- Robbins JD, Norred WP, Bathija A, Ulsamer AG (1984) “Bioavailability in rabbits of formaldehyde from durable-press textiles.” J Toxicol Environ Health 14:453-463.
- Sambrook, J, Fritsch, E.F, and Maniatis, T (1989) “Molecular Cloning: A Laboratory Manual.” Cold Spring Harbor Laboratory Press, NY, Vol. 1, 2, 3 .
- Sancar A. (1996) “DNA excision repair.“ Annu Rev Biochem.65:43-81.
- Sanderson BJ, Ferguson LR, Denny WA (1996) “Mutagenic and carcinogenic properties of platinum-based anticancer drugs.” Mutat Res. 355:59-70.
- Santagati F, Botta E, Stefanini M, Pedrini AM (2001) “Different dynamics in nuclear entry of subunits of the repair/transcription factor TFIIH.” Nucleic Acids Res. 29:1574-81.
- Sarasin A, Stary A (2007) “New insights for understanding the transcription-coupled repair pathway.” DNA Repair (Amst). 6:265-9.
- Satoh MS, Jones CJ, Wood RD, Lindahl T (1993) „DNA excision-repair defect of xeroderma pigmentosum prevents removal of a class of oxygen free radical-induced base lesions.“ Proc Natl Acad Sci USA 90:6335-9. :
- Shimomura O, Johnson FH, Saiga Y (1962) “Extraction, purification and properties of aequorin, a bioluminescent protein from the luminous hydromedusan, Aequorea.” J Cell Comp Physiol. 59:223-39.
- Shimomura O, Johnson FH, Saiga Y (1963) “Microdetermination of Calcium by Aequorin Luminescence“ Science. 140(3573):1339-1340.
- Shimomura (1979) “Structure of the chromophore of Aequorea green fluorescent protein” FEBS Letters 104 (220-22)
- Shivji MK, Podust VN, Hübscher U, Wood RD (1995) “Nucleotide excision repair DNA synthesis by DNA polymerase epsilon in the presence of PCNA, RFC, and RPA." Biochemistry. 34:5011-7.
- Shivji MK, Moggs JG, Kuraoka I, Wood RD (2006) “Assaying for the dual incisions of nucleotide excision repair using DNA with a lesion at a specific site.” Methods Mol Biol. 314:435-56.
- Shiyanov P, Nag A, Raychaudhuri P (1999) „ Cullin 4A associates with the UV-

damaged DNA-binding protein DDB.“ J Biol Chem. 274:35309-12.

- Siddik ZH (2003) “Cisplatin: mode of cytotoxic action and molecular basis of resistance.” Oncogene. 22:7265-79.
- Sugasawa K, Ng JM, Masutani C, Iwai S, van der Spek PJ, Eker AP, Hanaoka F, Bootsma D, Hoeijmakers JH (1998) „Xeroderma pigmentosum group C protein complex is the initiator of global genome nucleotide excision repair.“ Mol Cell. 2:223-32.
- Sugasawa K, Okamoto T, Shimizu Y, Masutani C, Iwai S, Hanaoka F (2001) “A multistep damage recognition mechanism for global genomic nucleotide excision repair.” Genes Dev. 15:507-21.
- Sugasawa K, Okuda Y, Saijo M, Nishi R, Matsuda N, Chu G, Mori T, Iwai S, Tanaka K, Tanaka K, Hanaoka F (2005) „ UV-induced ubiquitylation of XPC protein mediated by UV-DDB-ubiquitin ligase complex.“ Cell. 121:387-400.
- Sugasawa K (2009) “UV-DDB: a molecular machine linking DNA repair with ubiquitination.” DNA Repair (Amst). 8:969-72.
- Szarvas T, Szatloczky E, Volford J, Trezel L, Tyihak E, Rusznak I (1986) „Determination of endogenous formaldehyde level in human blood and urine by dimedone-14C radiometri method.“ J Rad Nucl Chem. 106:357-367
- Tang JY, Hwang BJ, Ford JM, Hanawalt PC, Chu G (2000) „Xeroderma pigmentosum p48 gene enhances global genomic repair and suppresses UV-induced mutagenesis.“ Mol Cell. 5:737-44.
- Tyihák E, Bocsi J, Timár F, Rácz G, Szende B. (2001) “Formaldehyde promotes and inhibits the proliferation of cultured tumour and endothelial cells.“ Cell Prolif. 34(3):135-41.
- van Hoffen A, Venema J, Meschini R, van Zeeland AA, Mullenders LH (1995) „Transcription-coupled repair removes both cyclobutane pyrimidine dimers and 6-4 photoproducts with equal efficiency and in a sequential way from transcribed DNA in xeroderma pigmentosum group C fibroblasts.“ EMBO J. 14:360-7.
- van Royen ME, Dinant C, Farla P, Trapman J, Houtsmuller AB (2009) FRAP and FRET methods to study nuclear receptors in living cells. Methods Mol Biol. 505:69-96.
- Vaughan TL, Stewart PA, Teschke K (2000) „Occupational exposure to

formaldehyde and wood dust and nasopharyngeal carcinoma.“ Occup Environ Med 57:376-384.

- Venema J, van Hoffen A, Karcagi V, Natarajan AT, van Zeeland AA, Mullenders LH (1991) “Xeroderma pigmentosum complementation group C cells remove pyrimidine dimers selectively from the transcribed strand of active genes.“ Mol Cell Biol. 11:4128-34.
- Vilaplana J, Romaguera C (2000) “Contact dermatitis from tosylamide/formaldehyde resin with photosensitivity.” Contact Dermatitis 42:311-312.
- Volker M, Moné MJ, Karmakar P, van Hoffen A, Schul W, Vermeulen W, Hoeijmakers JH, van Ariel R, van Zeeland AA, Mullenders LH (2001) “Sequential assembly of the nucleotide excision repair factors in vivo.“ Mol Cell. 8:213-24.
- Walrath J, Fraumeni JF (1983) “Mortality patterns among embalmers.” Int J Cancer 31:407-411.
- Wilkinson KD (2000) “Ubiquitination and deubiquitination: targeting of proteins for degradation by the proteasome.” Semin Cell Dev Biol. 11:141-8.
- Wood RD (1996) “DNA repair in eukaryotes.“ Annu Rev Biochem. 65:135-67.
- Wood RD (1997) “Nucleotide excision repair in mammalian cells.” J Biol Chem. 272:23465-8.
- Yang TT, Cheng L, Kain SR (1996) “Optimized codon usage and chromophore mutations provide enhanced sensitivity with the green fluorescent protein.” Nucleic Acids Res. 24:4592-3.
- Yano K, Morotomi-Yano K, Adachi N, Akiyama H (2009) “Molecular mechanism of protein assembly on DNA double-strand breaks in the non-homologous end-joining pathway.” J Radiat Res (Tokyo). 50:97-108.
- You JS, Wang M, Lee SH (2003) „Biochemical analysis of the damage recognition process in nucleotide excision repair.“ J Biol Chem. 278:7476-85.

8 ZUSAMMENFASSUNG

Die genetische Information wird ständig verschiedenen physikalischen und chemischen Einflüssen ausgesetzt, die zur Schädigung der DNA führen. Um das Genom zu schützen, prozessiert die Nukleotid-Exzisionsreparatur (NER) eine große Vielfalt von nicht verwandten DNA-Addukten, einschließlich solche die zum Beispiel durch UV-Licht oder Cisplatin hervorgerufen werden. Das Ziel dieser Arbeit war, die entsprechenden Reparaturproteine mittels Fluoreszenz so zu markieren, dass deren Aktivität in lebenden Fibroblasten untersucht werden kann. Mit dieser Methode soll die Wirkung von Formaldehyd, ein weit verbreitetes genotoxisches Agens, auf die NER-Reaktion geprüft werden. Für die Bestimmung der intrazellulären Aktivität der Reparaturproteine wurden die Kinetik ihrer Ansammlung an Schadstellen und ihre Dynamik in „fluorescence recovery“ Experimenten ermittelt. Diese Echtzeit-Untersuchungen ergaben, dass Formaldehyd schon in niedrigen, nicht-zytotoxischen Konzentrationen die nukleäre Beweglichkeit der XPC- und DDB2-Erkennungsproteine einschränkt, womit ihre Rekrutierung an Schadstellen verlangsamt wird. Weitere Echtzeit-Versuche mit fluoreszenzmarkiertem Ubiquitin weisen darauf hin, dass DDB2 die Protein-Ubiquitylierung in Folge der Einwirkung von Formaldehyd stimuliert. Somit zeigen unsere Untersuchungen, dass formaldehydinduzierte Vernetzungen die Aktivität der NER-Faktoren behindern und auf dieser Weise die Exzisionsreparatur von mutagenen DNA-Schäden beinträchtigen.

9 ACKNOWLEDGMENTS

I would like to express my thanks to:

Dr. Ulrike Camenisch for thesis supervision, critical advice and continuous support in the experimental work. Also for being more than a supervisor and for proofreading my manuscript.

Prof. Dr. Hanspeter Naegeli for helpful discussions and the Referat.

PD Dr. Andreas Luch for the Koreferat.

Prof. Dr. Felix R. Althaus who gave me the opportunity to do my doctoral thesis at the institute of veterinary pharmacology and toxicology.

The Center for Microscopy and Image Analysis (ZMB) in particular Dr. Urs Ziegler, Caroline Aemisegger and Claudia Dumrese for their technical support for the FRAP experiments and their patience with me.

All my colleagues at the institute for helpful discussion and tips for experimental work. In particular I would thank Catherine and Basil for having pleasant lunch times and Flurina for quicker understanding of swiss german.

My special thanks go to my parents, my sister and her family, my grandmother and my aunt and uncle for their unfailing support and encouragement in whatever I am doing.

And finally, I want to thank Micha for coming to Zurich, his supporting in every instance and the Jungfaujoch.

CURRICULUM VITAE

Name	Renée Müller
Date of birth	March 7th 1983
Place of birth	Hoyerswerda
Nationality	German

1989 – 1993	1. Grundschule „Am Adler“, Hoyerswerda, Germany
1993 – 2001	Lessing-Gymnasium, Hoyerswerda, Germany
2001	graduation: Abitur
2001 – 2007	Faculty of Veterinary Medicine, University of Leipzig, Leipzig, Germany
2003 – 2004	School of Veterinary Medicine, Vetsuisse Faculty, University of Zürich, Zürich, Switzerland
2005 – 2007	Degree in Veterinary Medicine, University of Leipzig, Leipzig, Germany
2007 – 2008	Doctoral thesis work at the Institute of Veterinary Pharmacology and Toxicology, Vetsuisse Faculty, University of Zürich, Zürich, Switzerland
Since 2009	Veterinarian in a small animal clinic, Weißwasser, Germany